



NAM

Special Report on the Garrelsweer Earthquake 16th November 2021 with Magnitude $M_L = 3.2$

Datum November 2021

Editors Jan van Elk and Jeroen Uilenreef

Contents

Summary and Conclusions	5
Ground Motion Comparison	5
Seismological Comparison.....	5
1 Introduction	6
1.1 Reason for this Special Report.....	6
1.2 Content of this Special Report.....	7
2 Analysis of the recorded surface ground-motions	8
2.1 Introduction	8
2.2 Peak Ground Accelerations and Velocities	10
2.3 Ground-Motion Durations	15
2.4 Spectral Accelerations and Comparison with Ground-Motion Models.....	18
2.5 Concluding Remarks	22
3 Chance of an earthquake with a magnitude $M_L \geq 3.2$	23
4 References	25
Appendix A Evaluation of observed ground motions for the earthquake Zeerijp earthquakes based on GMM V6	26
Appendix B Evaluation of the hypocentre and the source mechanism of the earthquake with a magnitude of 3.2 near Garrelsweer on 16 th November	29

Summary and Conclusions

Ground Motion Comparison

The M_L 2.5 Garrelsweer earthquake of 16th November 2021 has generated a large number of ground-motion recordings. The largest component of PGA recorded in this earthquake is $0.03g$, which is significantly smaller than the largest PGA values recorded in Groningen ($0.11g$ in the 8th January 2018 M_L 3.4 Zeerijp earthquake and $0.08g$ in the 16th August 2012 Huizinge earthquake). The largest value of PGV—which is generally considered a better indicator of the damage potential of the motion—recorded in this latest event is just 1.58 cm/s, which is less than half of the largest value of the Groningen ground-motion database, a 3.46 cm/s recorded in the Huizinge earthquake.

An important observation is that the motions recorded in the Garrelsweer earthquake are consistent with the predictions from the ground-motion model currently deployed in the seismic hazard and risk modelling for Groningen and the empirical PGV GMPEs used to assess damage claims.

Seismological Comparison

Using the seismological model, the exceedance probability for an earthquake with magnitude $M_L \geq 3.2$ has been calculated for an average temperature year. For gas-year 2020/2021 this exceedance probability is 20.34% and for gas-year 2021/2022 it is 16.67 %. For calendar year 2021 the exceedance probability is 18.64%.

The occurrence of an earthquake with the magnitude $M_L = 3.2$, like the Garrelsweer earthquake, is therefore within the predictive band for the seismological model supporting SDR-2021 (and the Operational Strategy for 2021/2022) and is based on this model not an exceptional occurrence.

The Garrelsweer earthquake was followed by a series of much smaller earthquakes in the same area. In combination with the Zeerijp earthquake swarm starting on 4th October 2021, this might indicate a more intense clustering of recent earthquakes in space and time. However, this might also be associated with a lower event rate and a shrinking seismically active area. NAM will therefore carry a systematic search in the Groningen earthquake catalogue for after-shock sequences.

1 Introduction

1.1 Reason for this Special Report

When larger earthquakes have occurred or other remarkable events have happened (like a swarm of smaller earthquakes), NAM published a report within two weeks after the event. To date twelve of these reports have been published. These reports are listed in table 1.1.

Title	Date
Rapportage recente aardbevingen Wirdum en Garsthuizen 2016/2017	Mar 2017
Ground Motions from the M_L 2.6 Slochteren Earthquake of 27 th May 2017	June 2017
Special Report on the earthquake density and activity rate following the earthquakes in Appingedam ($M_L=1.8$) and Scharmer ($M_L=1.5$) in August 2017	Sept 2017
Special Report on the Loppersum earthquakes – December 2017	Dec 2017
Special Report on the Zeerijp Earthquake	Jan 2018
Short special report Exceedance Activity Rate - February 2018	Feb 2018
Special Report - Westerwijdwerd Earthquake - 22 nd May 2019	May 2019
Analyse overschrijding MRP-grenswaarde Aardbevingsdichtheid 9 september 2019	Sept 2019
Analyse overschrijding aardbevingsdichtheid - 3 december 2019	Dec 2019
Special Report on the Zijldijk $M_L = 2.5$ Earthquake of 2 nd May 2020	May 2020
Special Report on the Loppersum $M_L=2.7$ earthquake of 14 th June 2020	August 2020
Special Report on the Zeerijp Earthquake Swarm starting 4 th October 2021	Nov 2021

Table 1.1 Reports analysing remarkable events in the earthquake record, like larger events or earthquake swarms.

The earthquake near Garrelsweer on the 16th November 2021 had a magnitude of 3.2 on the Richter-scale. As a result the 'signaalwaarde' for magnitude was exceeded. This exceedance requires NAM to submit a Special Report. Prior to the exceedance of the 'signaalwaarde' for magnitude, the monitoring level for earthquake density was exceeded on the 8th November 2021. For this a special report has been prepared and shared with both SodM and the ministry of Economic Affairs and Climate Policy .

Title	Date
Analyse seismiciteit	Nov 2016
Rapportage Seismiciteit Groningen - November 2017	Nov 2017
Rapportage Seismiciteit Groningen - Juni 2018	July 2018
Rapportage Seismiciteit Groningen - November 2018	Nov 2018
Rapportage Seismiciteit Groningen - Mei 2019	May 2019
Rapportage Seismiciteit Groningen - November 2019	Nov 2019
Rapportage Seismiciteit Groningen - Mei 2020	Apr 2020
Rapportage Seismiciteit Groningen - November 2020	Nov 2021
Rapportage Seismiciteit Groningen - Mei 2021	June 2021
Rapportage Seismiciteit Groningen - November 2021	Nov 2021

Table 1.2 Half-yearly surveillance reports issued by NAM to SodM and published on the NAM onderzoeksrapporten-webpage.

The half-yearly seismic monitoring report for November 2021 (Table 1.2) was submitted to SodM and the ministry of Economic Affairs and Climate Policy together with the Special Report on the Zeerijp earthquake swarm.

1.2 Content of this Special Report

In this report the earthquake records obtained during the Garrelsweer earthquake are discussed (chapter 2). In chapter 3 a seismological analysis of the Garrelsweer earthquake is provided.

The automated FWI analysis of the Garrelsweer earthquake of 16th November 2021 with a magnitude of 3.2 has been included in this report as Appendix A.

2 Analysis of the recorded surface ground-motions

2.1 Introduction

On Tuesday 16 November 2021 at 00:46 UTC (01:46 pm local time), an earthquake of local magnitude (M_L) of 3.2 occurred near the village of Garrelsweer, in the northern part of the Groningen field (Figure 2.1). The epicentral coordinates (245690 X, 592380 Y) depicted in Figure 2.1, and a focal depth of 2.85 km, were calculated by Dr Jesper Spetzler of KNMI using the 3D EDT method (Spetzler & Dost, 2017).

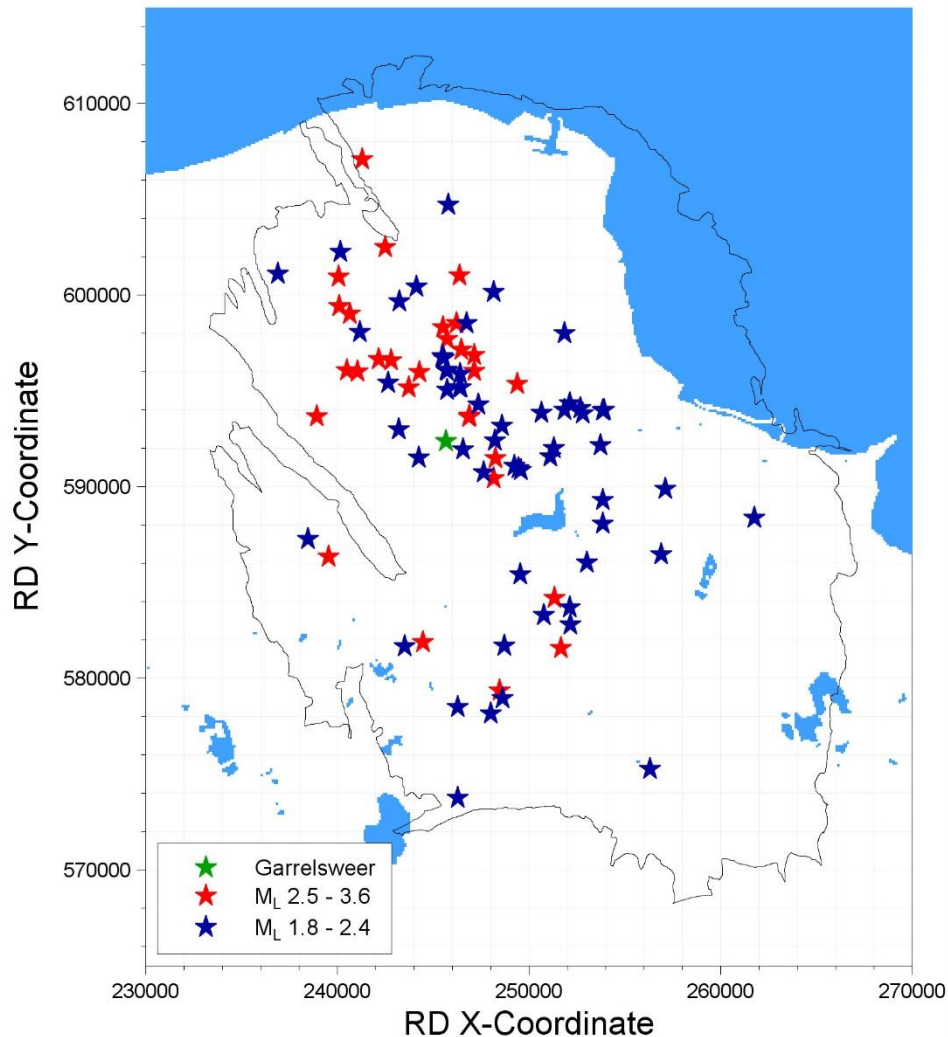


Figure 2.1 Epicentre of Garrelsweer earthquake (green star) together with epicentres of previous earthquakes of $M_L \geq 2.5$ (red stars) and of $M_L 1.8 - 2.4$ (blue stars)

The last event with a magnitude equal or larger to $M_L 2.5$ —the smallest magnitude considered in the Groningen Seismic Hazard & Risk Assessment— was the $M_L 2.5$ Zeerijp earthquake of 4th October 2021. Only four out of the other 30 $M_L \geq 2.5$ events have had a larger magnitude, with the latest being the $M_L 3.4$ Westerwijtwerd earthquake of 22nd May 2019. In keeping with trend during recent earthquakes (Figure 2.2) following the expansion of the strong-motion recording networks in the Groningen field (Dost *et al.*, 2017; Ntinalexis *et al.*, 2019), the latest earthquake has triggered a large number of accelerograms. This is the fourth event of magnitude equal to 3.2 to be recorded in Groningen but with only one occurring after the network expansion. Furthermore, it is the third largest event that has been recorded by the expanded networks to date.

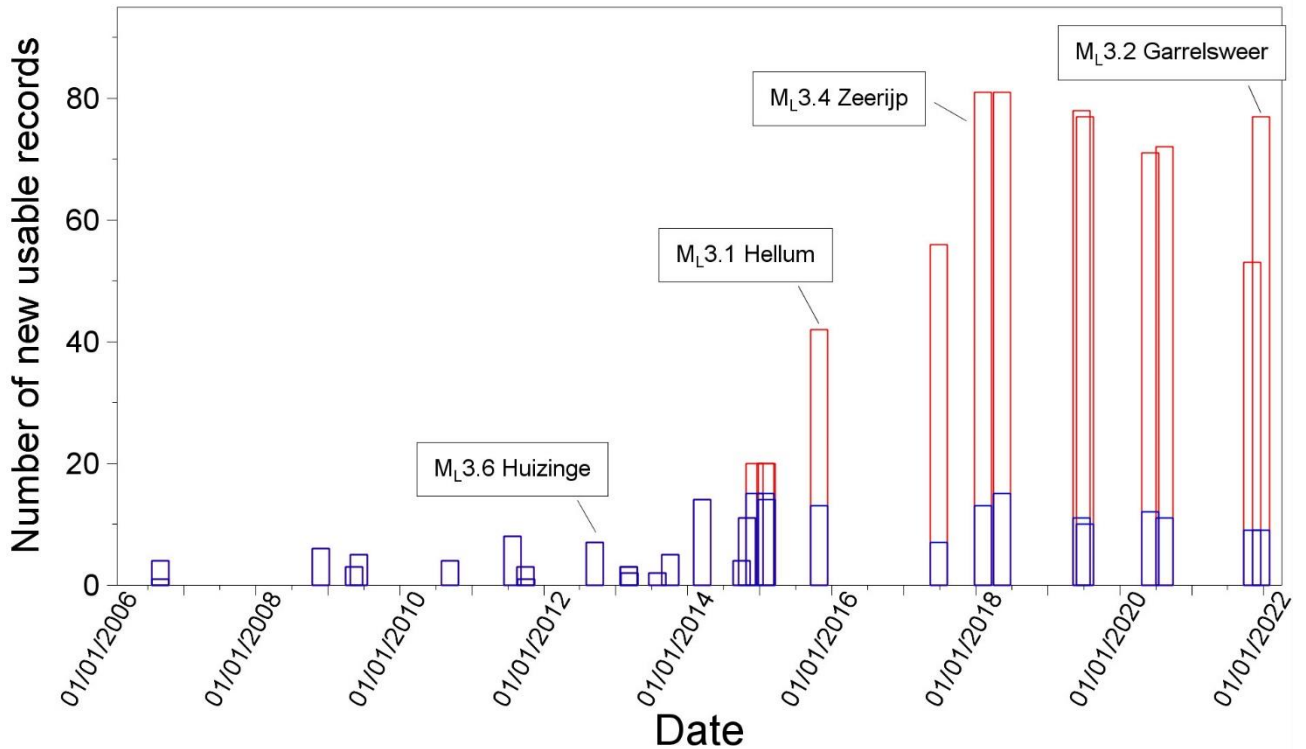


Figure 2.2 Diagram illustrating the timing of earthquakes of $M_L \geq 2.5$ in the Groningen field since 2006 and the number of records yielded by the permanent KNMI network (B-stations, blue) and by the expanded borehole geophone network (G-stations, red).

The KNMI portal (<http://rdsa.knmi.nl/dataportal/>) made accelerograms from the earthquake available within an hour of the event and 81 three-component recordings from the surface stations of the KNMI B- and G-networks were downloaded for this preliminary assessment of the motions. The records were processed as described by Edwards & Ntinalexis (2021) and a total of 77 records were deemed usable. Figure 2.3 shows the usable recordings in the magnitude-distance occupied by the database used to derive the current empirical ground-motion prediction equations (GMPEs) used to estimate values of peak ground velocity (PGV) occurring during earthquakes in the Groningen field (Bommer *et al.*, 2021b). This report presents an overview of the recorded motions from the Garrelsweer event in terms of their amplitudes and durations, and discusses how the recorded amplitudes of motion compare with predictions from the empirical PGV GMPE and the V7 Ground-Motion Model (GMM; Bommer *et al.*, 2021a). The discussions focus primarily on peak ground acceleration (PGA), which is assumed equal to the spectral acceleration at a period of 0.01 seconds, and PGV, which has been shown to correlate very well with the spectral acceleration at a period of 0.3 seconds for the Groningen data (Figure 2.4).

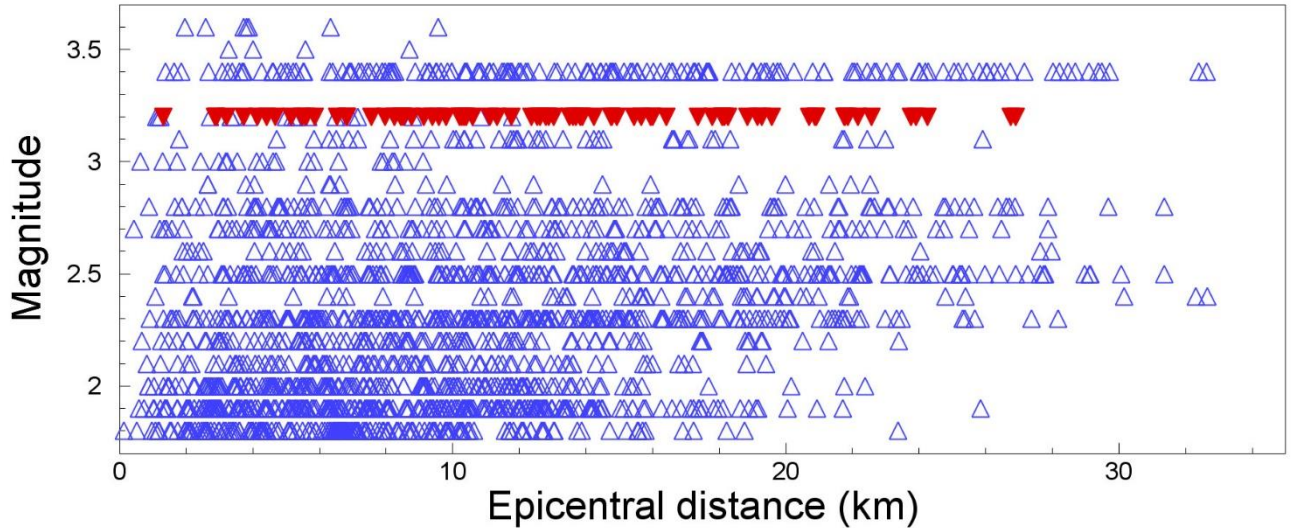


Figure 2.3 Magnitude-distance distribution of the Groningen strong-motion database including the recordings of the 16 November 2021 Garrelsweer earthquake.

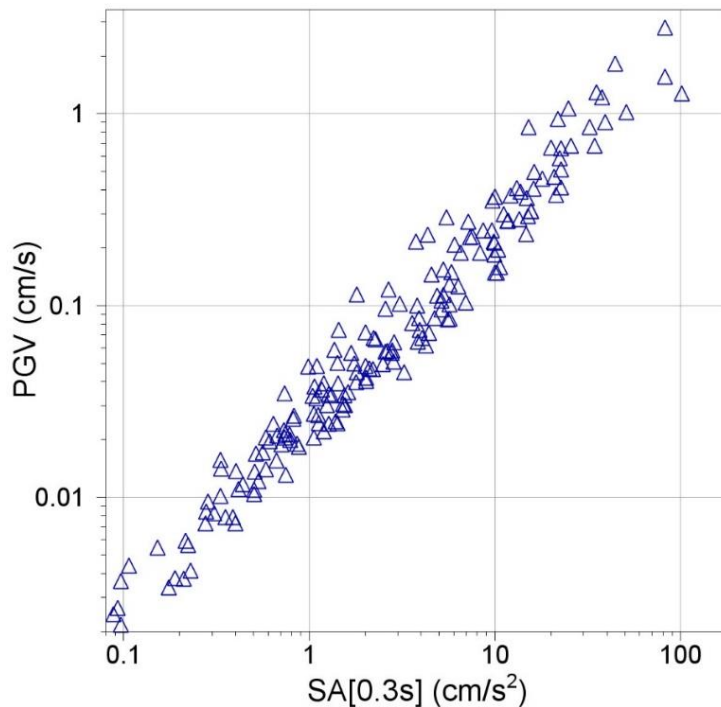


Figure 2.4 Correlation between values of PGV and spectral accelerations at 0.3 seconds for the Groningen strong-motion database (Bommer et al., 2017b).

2.2 Peak Ground Accelerations and Velocities

Figures 2.5 and 2.6 show the horizontal values of PGA and PGV of three component definitions from each recording obtained during the Garrelsweer earthquake plotted against the distance of the recording site from the epicentre. The largest amplitude was obtained at the G180 station located 2.9 km from the epicentre: the PGA recorded at the H2 (EW) component of this station is 33.32 cm/s^2 . The second largest PGA value was recorded at station G230 and 1.31 km from the epicentre: 24.70 cm/s^2 on the H2 (EW) component. The largest PGV value was also at the H2 (EW) component of station G230 and is 1.58 cm/s , while the second largest PGV value was recorded at the H2 (EW) component of G180: 1.11 cm/s .

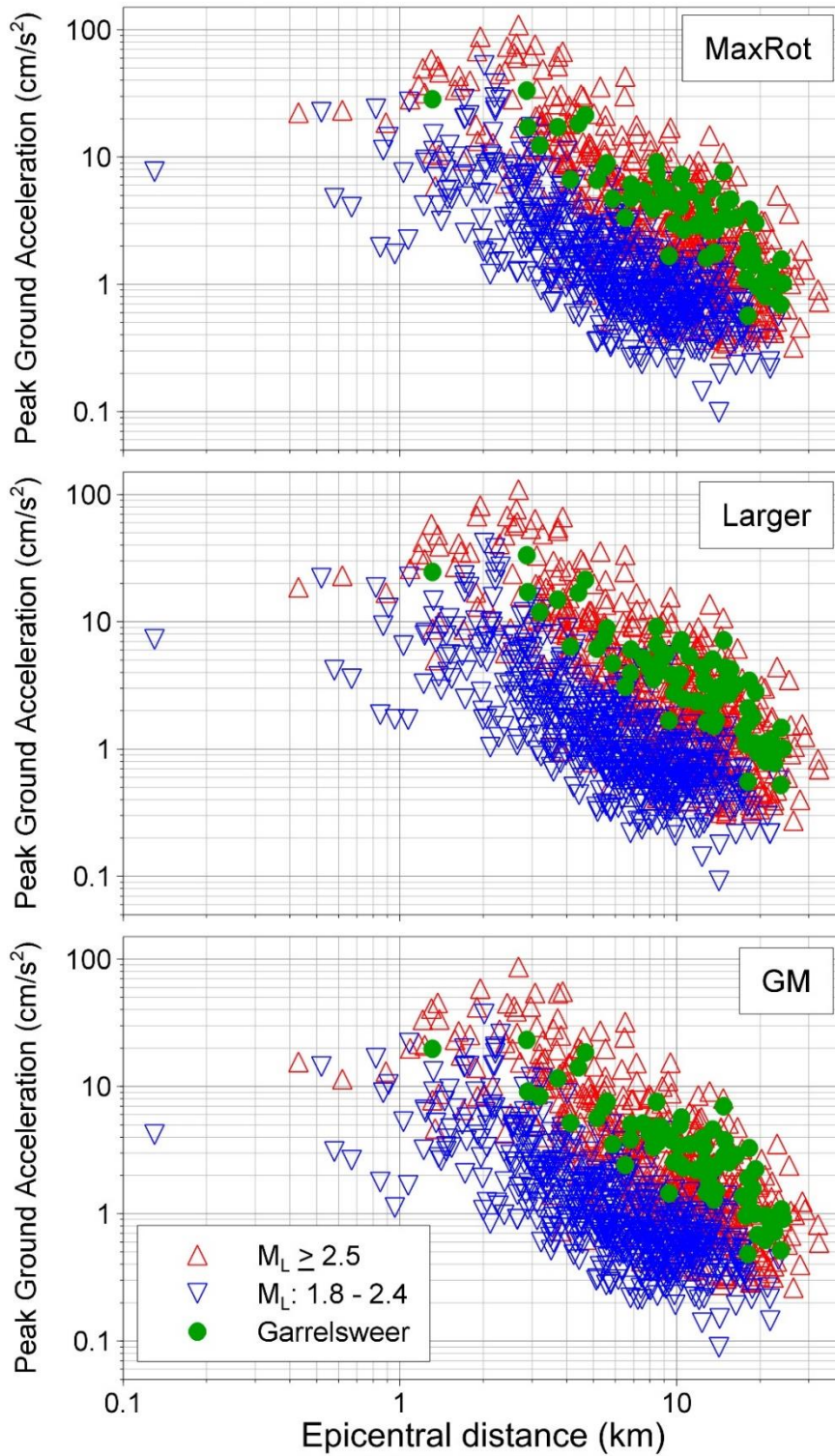


Figure 2.5 Horizontal components of PGA recorded during the Garrelsweer earthquake and previous earthquakes plotted against epicentral distance.

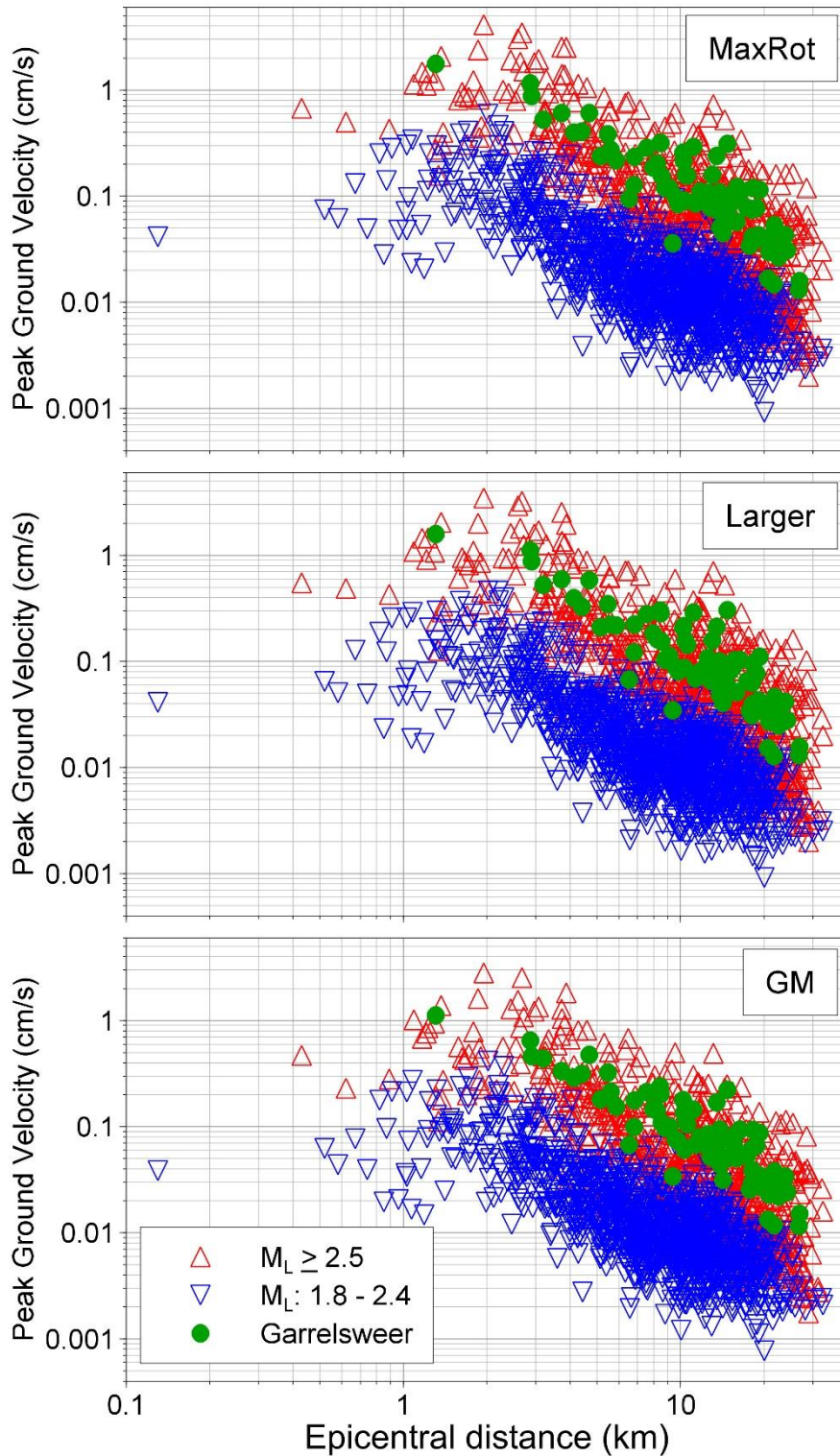


Figure 2.6 Horizontal components of PGV recorded during the Garrelsweer earthquake and previous earthquakes plotted against epicentral distance.

From Figures 2.5 and 2.6 it is immediately apparent that the amplitudes of motion are consistent with previous earthquakes of comparable size. Figure 2.7 shows the horizontal components of PGA and PGV obtained within 6 km of the epicentre, from which it can be appreciated that the very strong polarisation often observed in Groningen recordings (e.g., Bommer *et al.*, 2017a) is also apparent in records of this event.

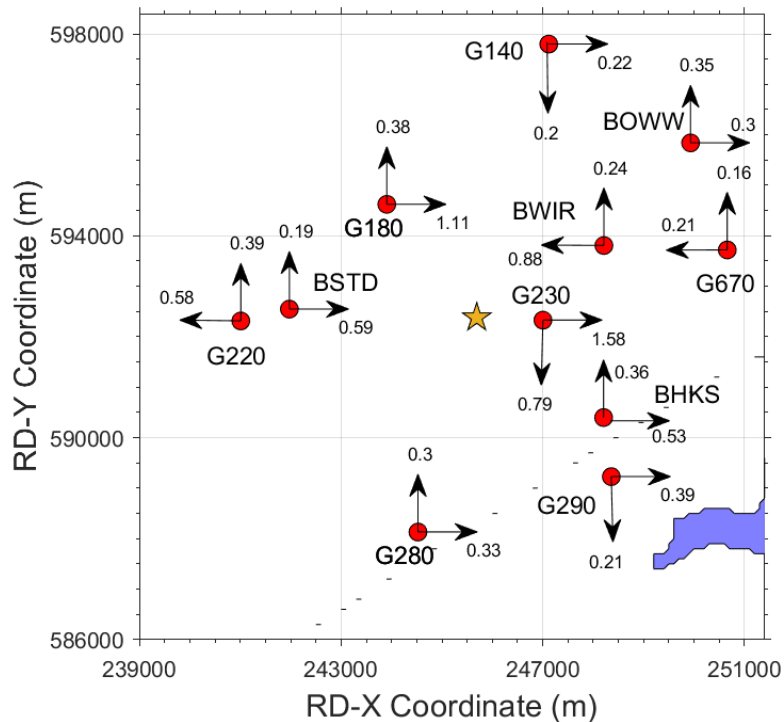
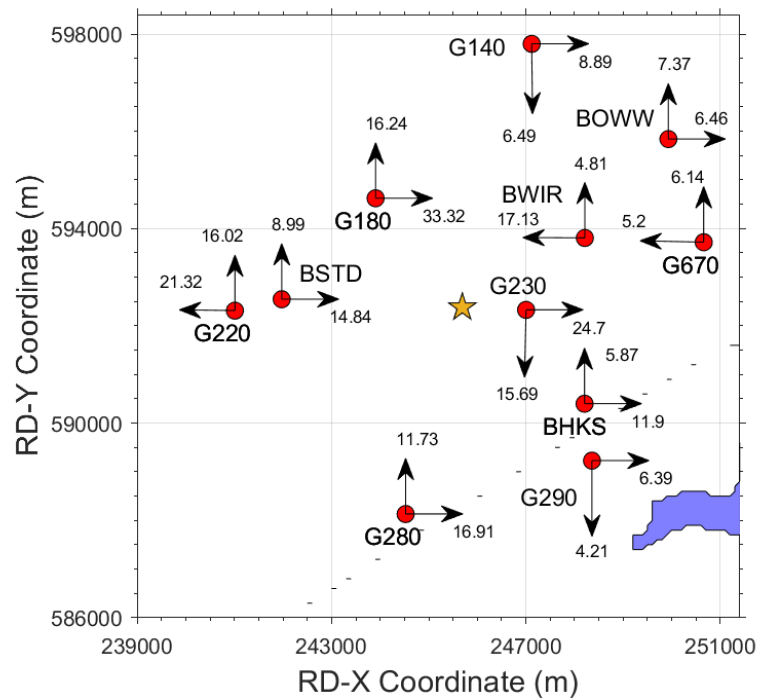


Figure 2.7 Horizontal components of PGA (upper) and PGV (lower) recorded during the Garrelsweer earthquake at epicentral distances of less than 6 km; units are cm/s² and cm/s, respectively.

As already shown in Figures 2.5 and 2.6, the amplitudes decay rapidly with distance although the effect of simultaneous arrivals of direct and critically refracted/reflected waves leads to an increase in amplitudes at some locations between 12 and 20 km from the epicentre. However, these effects do not lead to significant absolute amplitudes at those distances, and it is clear from Figure 2.7 that outside the epicentral area, the motions are of low amplitude: < 0.01g for PGA and < 0.2 cm/s for PGV.

Overall the motions appear similar to those observed in previous earthquakes. Figure 2.8 shows the geometric mean horizontal components of PGA and PGV plotted against magnitude together with the corresponding values from the complete database.

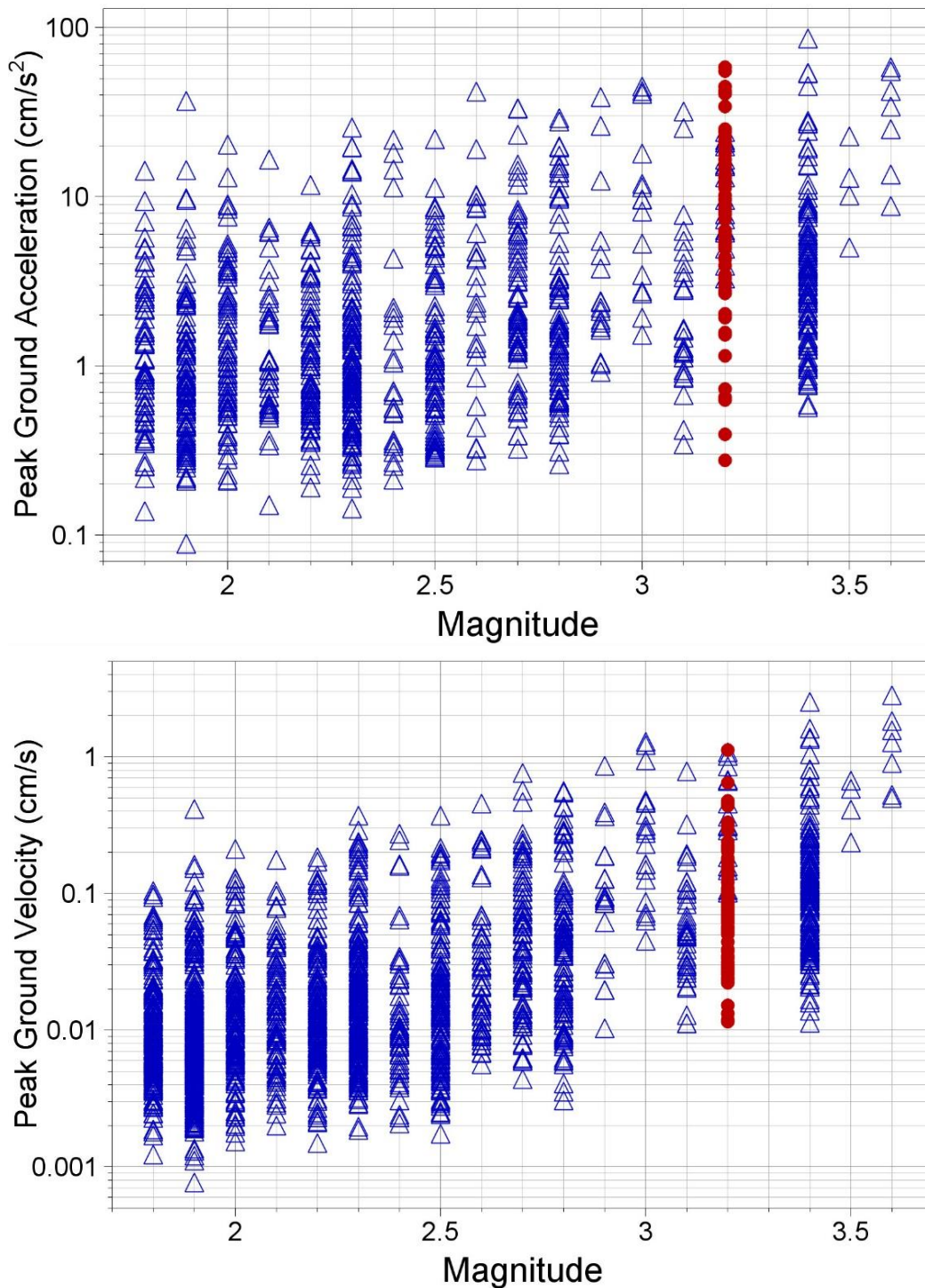


Figure 2.8 Geometric mean horizontal components of PGA (upper) and PGV (lower) recorded during the Garrelsweer earthquake (red) and in previous earthquakes (blue) plotted against local magnitude.

2.3 Ground-Motion Durations

The maximum amplitude of ground shaking, whether represented by PGA or PGV, provides a simple indication of the strength of the motion but the potential for adverse effects—such as damage to masonry buildings or triggering liquefaction—also depends on the duration or number of cycles of the motion.

A feature that has been consistently observed in the Groningen ground motions is a very pronounced negative correlation between PGA and duration, with high amplitude motions consistently associated with shaking of very short duration (Bommer *et al.*, 2016). The same pattern is observed in the recordings of the Garrelsweer earthquake, as shown in Figure 2.9. The larger amplitude component of the G230 recording—the closest station to the epicentre and source of the second and third largest PGA values—is associated with a significant duration of only 0.61 s. The horizontal components of both acceleration and velocity from this station are shown in Figure 2.10, which also shows the build-up of Arias intensity (which is a measure of the energy in the motion) over time. The strong concentration of the energy in a single pulse of motion in the H2 component is immediately apparent. On the other hand, the largest value of PGA, recorded on the H2 (EW) component at the G180 station, is associated with a duration larger than two seconds (2.255 s). The concentration of the energy in a single pulse can also be observed for this record (Figure 2.11), however its duration is elongated by a strong P-wave arrival approximately one second before the time of the acceleration peak.

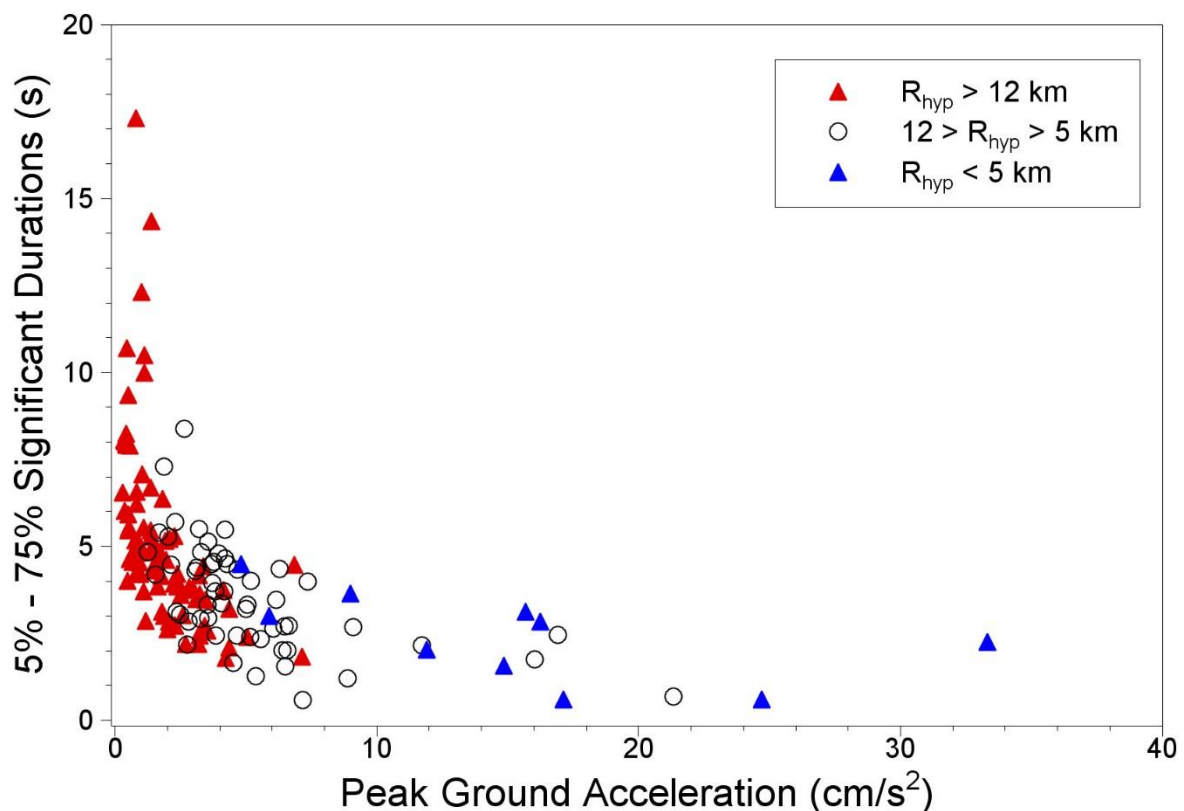


Figure 2.9 Pairs of PGA and significant duration for individual components of the Garrelsweer records, with symbols indicating the rupture distance of the recording.

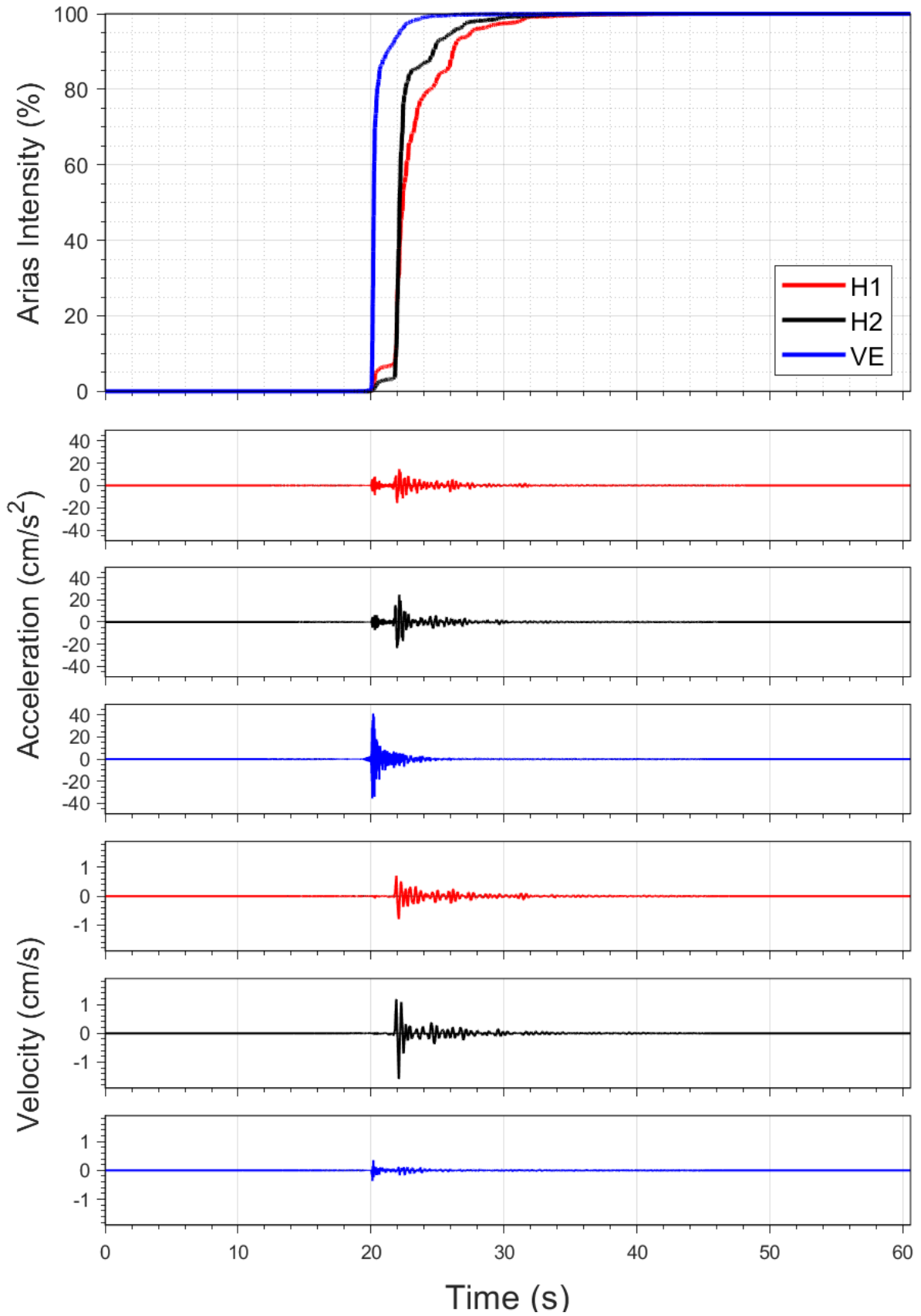


Figure 2.10 Horizontal components of acceleration and velocity from the G230 station; the upper frame shows the accumulation of Arias intensity (energy) over time.

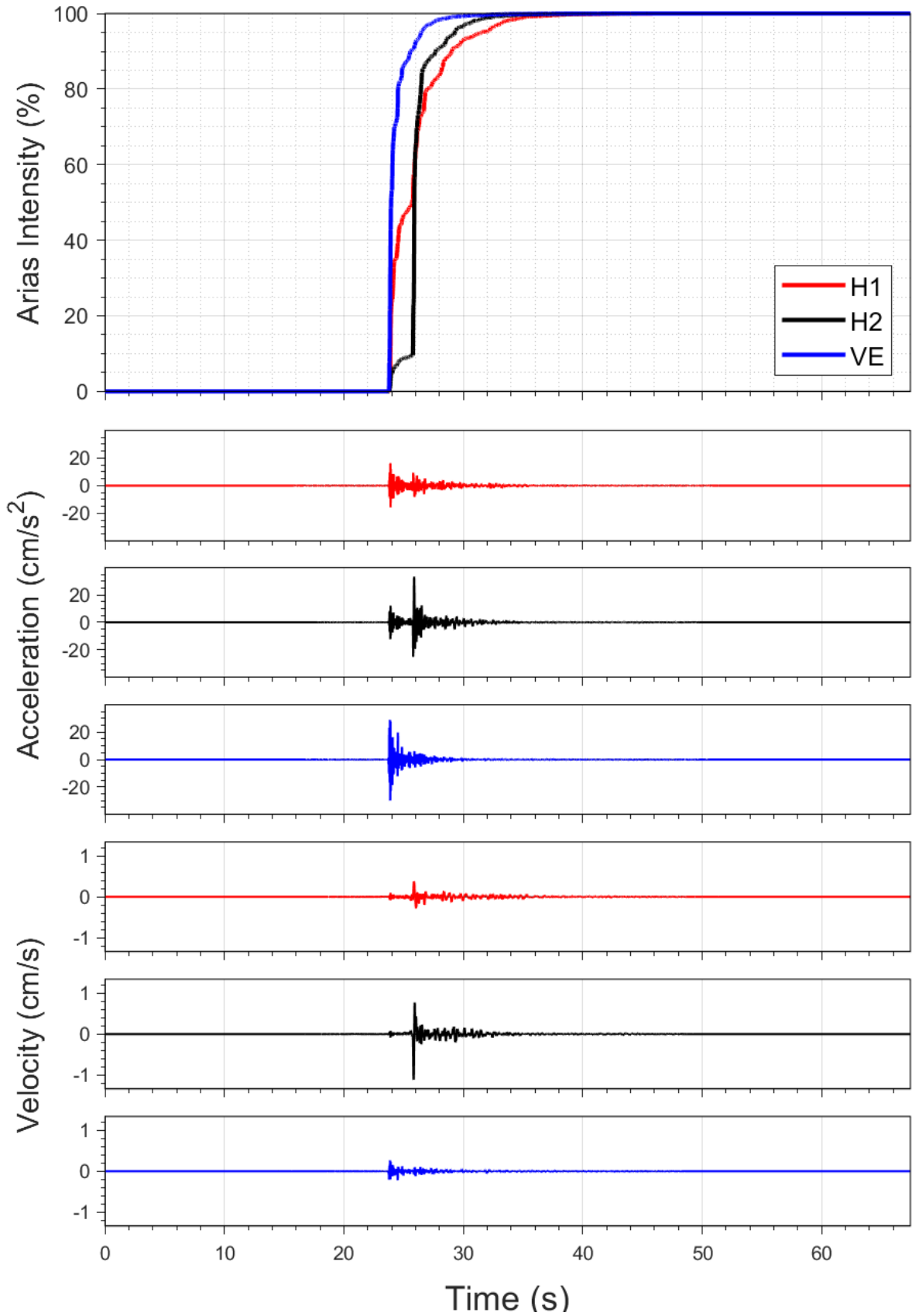


Figure 2.11 Horizontal components of acceleration and velocity from the G180 station; the upper frame shows the accumulation of Arias intensity (energy) over time.

2.4 Spectral Accelerations and Comparison with Ground-Motion Models

Additional insight into the nature of the ground motions can be obtained from the 5%-damped acceleration response spectra. The horizontal acceleration response spectra from the G180 and G230 recordings of the Garrelsweer earthquake are shown in Figure 2.12. The spectral shapes are consistent with previous observations in the field. The divergence between the red and black curves in both frames shows that the horizontal polarisation of both recordings seen for PGA and PGV (Figure 2.7) persists across the entire range of usable response periods, except between 0.025 – 0.05 seconds for G180 and between 0.017 – 0.022 seconds for G230. In the case of record G180, this reversal is observed because the peak of the acceleration of the H1 component is due to a P-wave arrival (Figure 2.10). P-waves have significant high-frequency content, resulting to a peak in the very short periods of the pseudo-acceleration response spectra. This can be clearly observed also in the spectra of the vertical components, which are always dominated by P-waves. Consistently with observations during previous events (Bommer *et al.*, 2017b), the vertical components display amplitudes which are large in comparison to the horizontal components.

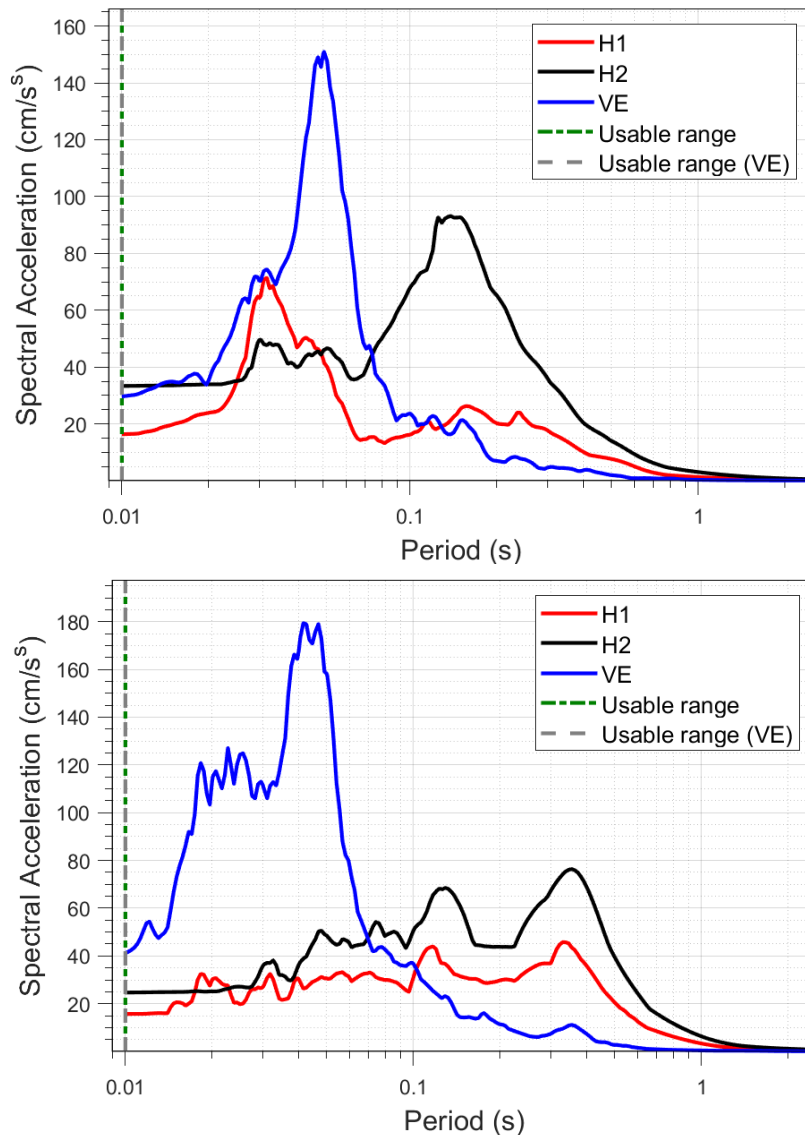


Figure 2.12 Horizontal response spectra from the G180 (upper) and G230 (lower) stations; vertical spectra plotted as dashed lines beyond maximum usable period.

For this preliminary analysis, the key question of interest is whether the motions recorded in this earthquake are consistent with the current GMM and empirical PGV GMPEs being used in the Groningen field. The current GMM is the V7 GMM, published in October 2021 (Bommer *et al.*, 2021a), and we have simply calculated the total residuals at the surface for different ground-motion parameters. In each case, the residual is the natural logarithm of the ratio of the observed (recorded) to the median predicted value, so a residual of 0.7 indicates that the recorded value was underestimated by a factor of 2 by the model and a residual of -0.7 would indicate over-prediction by a factor of 2.

Figure 2.13 shows the residuals of spectral accelerations at 0.01 seconds with respect to the V7 GMM plotted against rupture distance. The scatter is very considerable but, between the distances of 10 and 20 km, where there are more data from the latest event, it is similar to the scatter of the data used in the V7 GMM development. The residuals are centred fractionally above the zero line, which suggests a slight under-prediction by the model. At intermediate periods (Figures 2.14 and 2.15), the residuals are better centred on the zero line, indicating that the median predictions of the model provide an overall good fit to the data. Then, at longer periods (Figures 2.16 and 2.17), the residuals are centred below the zero line, indicating over-prediction by the model. The residuals of the event and the database have also been divided in six even logarithmic-distance bins, and the means of each bin are also presented in the Figures along with the associated 95% confidence intervals. In Figures 2.13 – 2.16, the means of the event’s residuals are similar to the means computed for the V7 GMM database residuals; moreover, the binned means of the database are within the 95% confidence intervals of the means of the Garrelsweer earthquake’s records, indicating a consistency in the fit of the data to the model. The first and last bin, where fewer data points are available, are exceptions. Then, at the period of one second (Figure 2.17), the mean binned residuals of the latest earthquake are systematically smaller than those of the V7 GMM database.

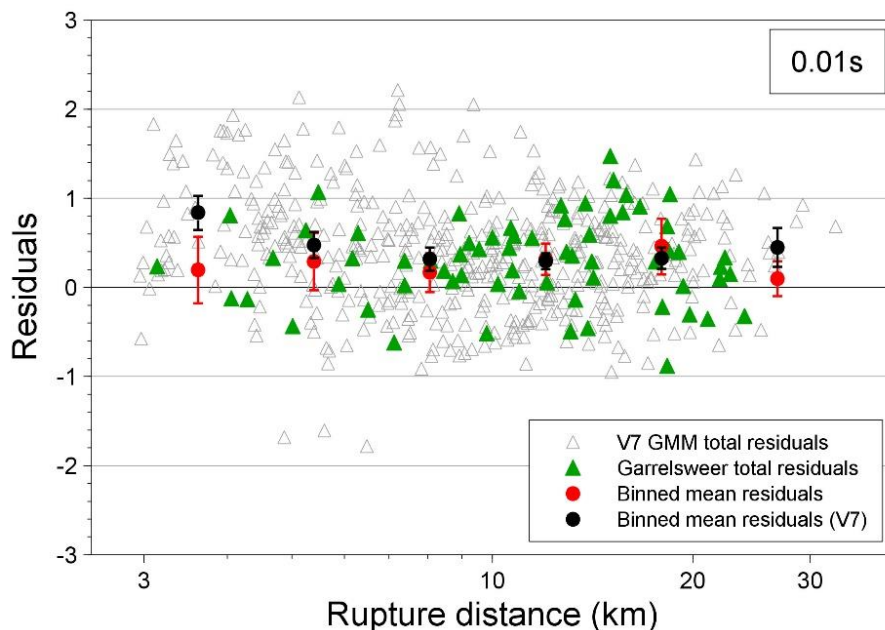


Figure 2.13 Residuals of $S_a(T)$ with respect to the central branch of the V7 GMM at 0.01 seconds.

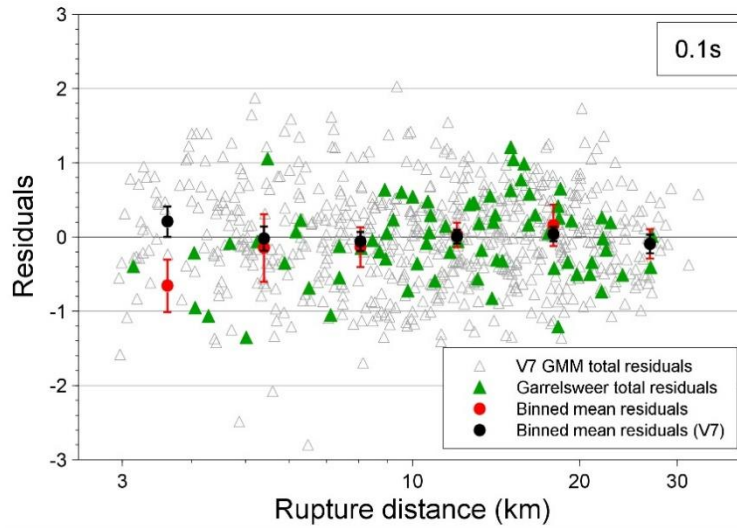


Figure 2.14 Residuals of $S_a(T)$ with respect to the central branch of the V7 GMM at 0.1 seconds.

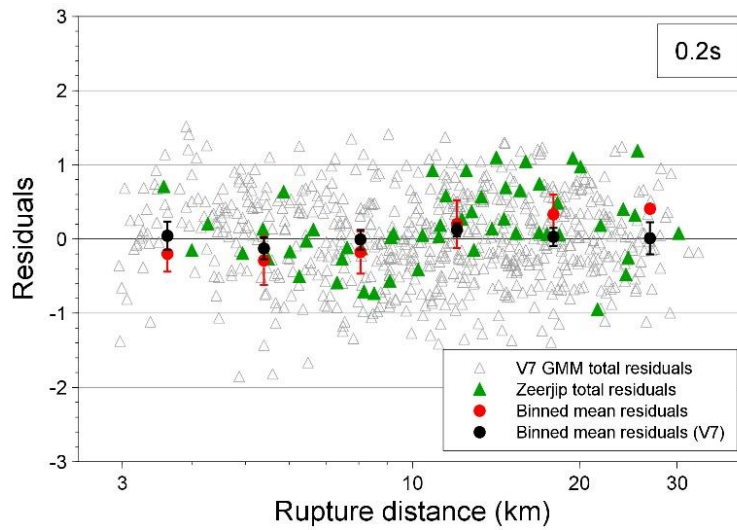


Figure 2.15 Residuals of $S_a(T)$ with respect to the central branch of the V7 GMM at 0.2 seconds.

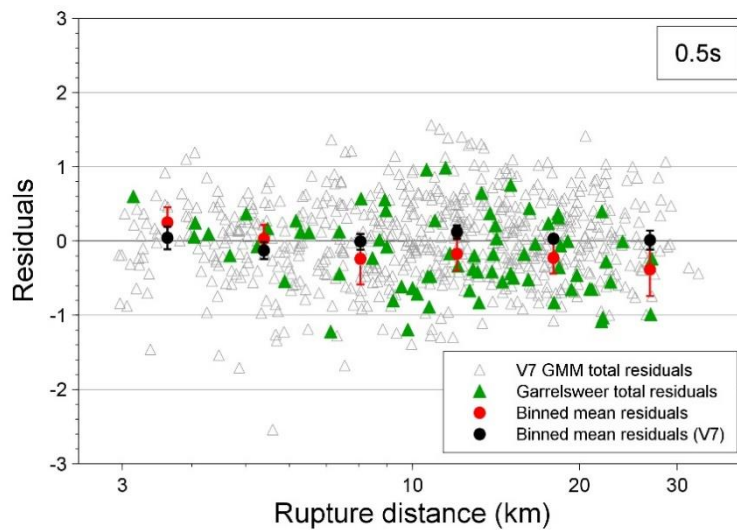


Figure 2.16 Residuals of $S_a(T)$ with respect to the central branch of the V7 GMM at 0.5 seconds.

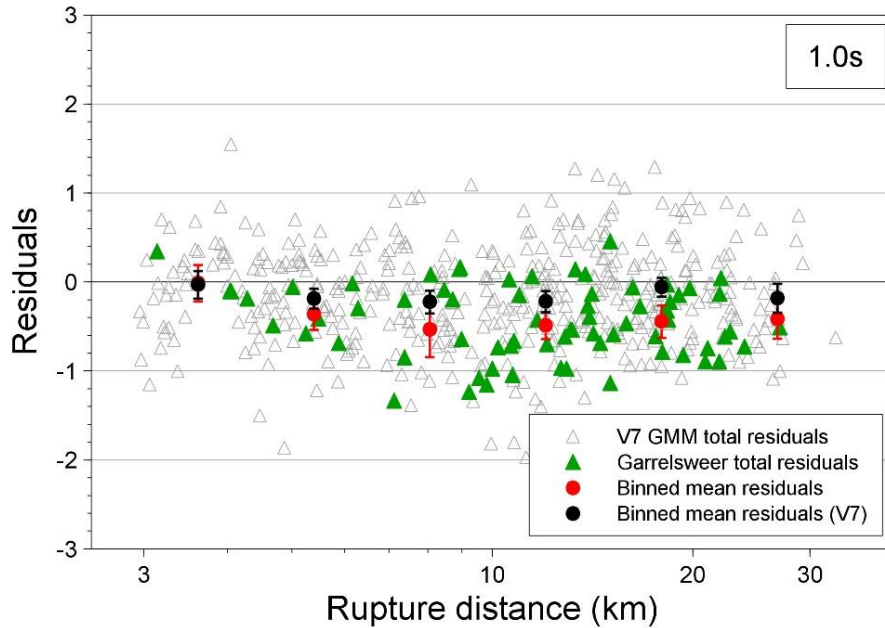


Figure 2.17 Residuals of $S_a(T)$ with respect to the central branch of the V7 GMM at 1 second.

The recent SDR-2021 was based on GMM V6. An evaluation of the ground motions based on GMM V6 is presented in appendix A.

The current empirical PGV model was also developed in 2021 (Bommer *et al.*, 2021b) and we have calculated the total, inter- and intra- event residuals. Figure 2.18 shows the intra-event residuals of three component definitions of PGV with respect to the empirical GMPE plotted against hypocentral distance. With two exceptions, nearly all residuals of the Garrelsweer earthquake recordings are within two within-event standard deviations of the zero line, which suggests that the model captures well the variability of the data.

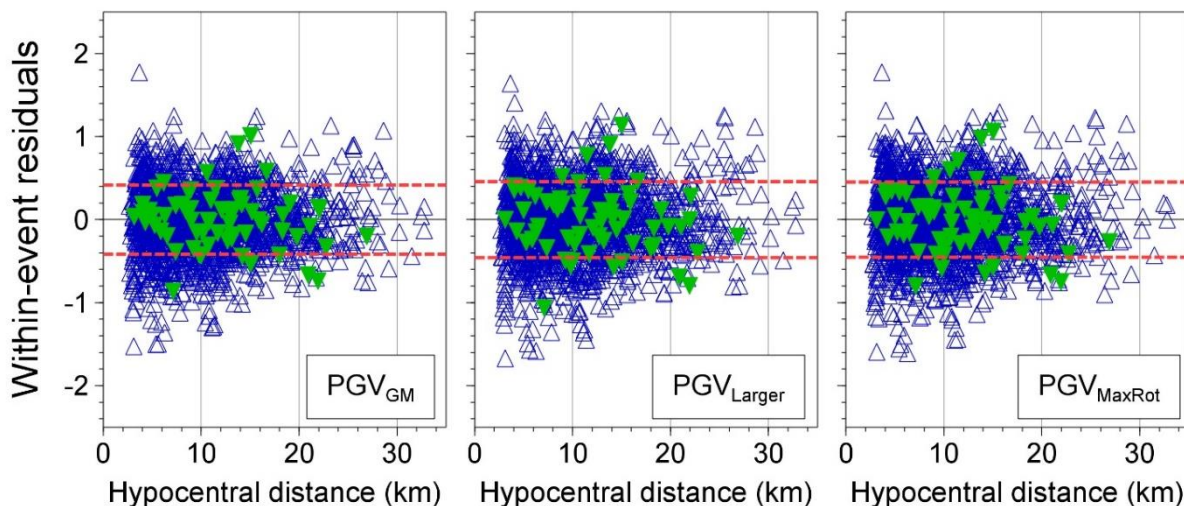


Figure 2.18 Event- and station-corrected within-event residuals of three component definitions of PGV with respect to the equations of the empirical PGV GMPE (Bommer *et al.*, 2021b). Residuals of the Garrelsweer earthquake recordings are shown in green and of other events in blue. The within-event standard deviation (φ_{ss}) is shown in red dashed lines.

Figure 2.19 compares the inter-event residuals (event-terms) of the Garrelsweer earthquake to those of the previous events of the database. These event terms effectively represent the average offset of

the recorded motions from each earthquake compared to the median prediction from the empirical model for the event magnitude, with a positive event-term indicating a stronger-than-average earthquake, a negative value a somewhat weaker-than-average earthquake. The event-term of the Garrelsweer earthquake has a negative value, equal to almost one inter-event standard deviation below zero, indicating that the PGV values recorded during this event are over-predicted by the medians of the GMPEs, and are smaller than what would be expected for an event of this magnitude.

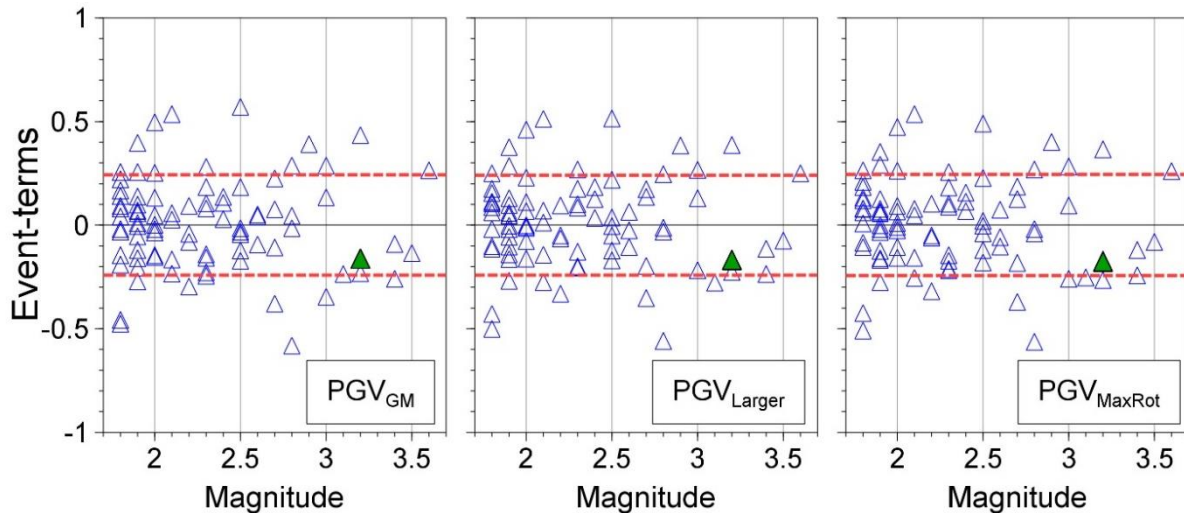


Figure 2.19 Inter-event residuals of three component definitions of PGV with respect to the equations of the empirical PGV GMPE (Bommer et al., 2021b). Residuals of the Garrelsweer earthquake recordings are shown in green and of older events in blue. The inter-event standard deviation is shown in red dashed lines.

2.5 Concluding Remarks

The M_L 2.5 Garrelsweer earthquake of 16th November 2021 has generated a large number of ground-motion recordings. The largest component of PGA recorded in this earthquake is $0.03g$, which is significantly smaller than the largest PGA values recorded in Groningen ($0.11g$ in the 8 January 2018 M_L 3.4 Zeerijp earthquake and $0.08g$ in the 16 August 2012 Huizinge earthquake). The largest value of PGV—which is generally considered a better indicator of the damage potential of the motion—recorded in this latest event is just 1.58 cm/s , which is less than half of the largest value of the Groningen ground-motion database, a 3.46 cm/s recorded in the Huizinge earthquake.

An important observation is that the motions recorded in the Garrelsweer earthquake are consistent with the predictions from the ground-motion model currently deployed in the seismic hazard and risk modelling for Groningen and the empirical PGV GMPEs used to assess damage claims.

3 Chance of an earthquake with a magnitude $M_L \geq 3.2$

The SDRA report prepared by TNO contains a table with the exceedance probability for a selection of earthquake magnitudes for the coming ten gas-years. This table has been reproduced in figure 3.1. In an appendix of the TNO report, the same data is also provided for calendar years (table A.1 in the TNO report).

Tabel 3.1 Jaarlijkse verwachting van het aantal bevingen met magnitude gelijk aan of hoger dan $M_{1.5}$ ("Rate") en overschrijdingskansen voor een aantal geselecteerde magnitudes per gasjaar voor een gemiddeld temperatuurverloop. De eerste kolom geeft het gasjaar (*gas year – GY*) weer.

	Rate	M3.5	M3.6	M4.0	M4.5	M5.0
GY2021/2022	5.64	6.78%	5.15%	1.46%	0.20%	0.03%
GY2022/2023	4.98	6.02%	4.57%	1.30%	0.18%	0.03%
GY2023/2024	4.56	5.51%	4.18%	1.19%	0.16%	0.02%
GY2024/2025	4.18	5.06%	3.84%	1.09%	0.15%	0.02%
GY2025/2026	3.85	4.67%	3.54%	1.00%	0.14%	0.02%
GY2026/2027	3.53	4.28%	3.24%	0.91%	0.12%	0.02%
GY2027/2028	3.27	3.96%	2.99%	0.84%	0.11%	0.02%
GY2028/2029	3.03	3.66%	2.77%	0.78%	0.11%	0.02%
GY2029/2030	2.83	3.42%	2.58%	0.72%	0.10%	0.01%
GY2030/2031	2.66	3.21%	2.42%	0.68%	0.09%	0.01%

Figure 3.1 Reproduction of table 3.1 from report "Publieke Seismische Dreigings-en Risicoanalyse Groningen gasveld 2021 - TNO2021 R10441" prepared by TNO.

The lowest magnitude for which the exceedance probability is provided in this table is $M_L \geq 3.5$. Using the same supporting seismological model, the exceedance probability for an earthquake with magnitude $M_L \geq 3.2$ has been calculated for an average temperature year. For gas-year 2020/2021 this exceedance probability is 20.34% and for gas-year 2021/2022 it is 16.67%. For calendar year 2021 the exceedance probability is 18.64%.

The occurrence of an earthquake with the magnitude $M_L = 3.2$, as the Garrelsweer earthquake, is therefore within the predictive band for the seismological model supporting SDRA-2021 (and the Operational Strategy for 2021/2022) and is based on this model not an exceptional occurrence.

The Garrelsweer earthquake on the 16th November with a magnitude of $M_L = 3.2$, was followed by a number of much smaller earthquakes in the same area. Table 3.1 provides an overview of these earthquake events.

Location	Date	Time – UTC	Magnitude
Garrelsweer	15 Nov 2021	12:41:52	0.6
Garrelsweer	16 Nov 2021	00:46:48	3.2
Winneweer	16 Nov 2021	01:34:16	0.6
Garrelsweer	16 Nov 2021	04:38:04	0.2
Garrelsweer	16 Nov 2021	02:57:44	0.3
Winneweer	17 Nov 2021	18:25:28	0.9

Table 3.1 Earthquakes recorded by the Groningen seismic monitoring network in the period 15th to 17th November 2021.

The Zeerijp earthquake of 4th October was also followed by an earthquake swarm. This could potentially indicate that recent earthquakes are more clustered in space and time. In other words, larger earthquakes are recently more likely to be associated with a swarm of smaller earthquakes. However due to the lower event rate in recent years, earthquakes are more separated in time and earthquake swarms might be more easily recognized. On the other hand, due to the shrinking seismically active area, earthquakes occur closer together in space giving potentially the impression of more intense clustering. NAM will therefore carry a systematic search in the Groningen earthquake catalogue for after-shock sequences.

4 References

1. Bommer, J.J., B. Dost, B. Edwards, P.J. Stafford, J. van Elk, D. Doornhof & M. Ntinalexis (2016). Developing an application-specific ground-motion model for induced seismicity. *Bulletin of the Seismological Society of America* **106**(1), 158-173.
2. Bommer, J.J., B. Edwards, P.P. Kruiver, A. Rodriguez-Marek, P.J. Stafford, M. Ntinalexis, E. Ruigrok & B. Dost (2021a). *V7 Ground-Motion Model for Induced Seismicity in the Groningen Gas Field*. Revision 1, 29 September 2021, 273 pp.
3. Bommer, J.J., P.J. Stafford, B. Edwards, B. Dost, E. van Dedem, A. Rodriguez-Marek, P. Kruiver, J. van Elk, D. Doornhof & M. Ntinalexis (2017a). Framework for a ground-motion model for induced seismic hazard and risk analysis in the Groningen gas field, The Netherlands. *Earthquake Spectra* **33**(2), 481-498.
4. Bommer, J.J., B. Dost, B. Edwards, P.P. Kruiver, P. Meijers, M. Ntinalexis, A. Rodriguez-Marek, E. Ruigrok, J. Spetzler & P.J. Stafford (2017b). *V4 Ground-Motion Model (GMM) for Response Spectral Accelerations, Peak Ground Velocity, and Significant Durations in the Groningen Field*. Version 2.1, 23 June 2017, 541 pp.
5. Bommer, J. J., P. J. Stafford, and M. Ntinalexis (2021b). Empirical Equations for the Prediction of Peak Ground Velocity due to Induced Earthquakes in the Groningen Gas Field, 10 March 2019
6. Dost, B., E. Ruigrok & J. Spetzler (2017). Development of probabilistic seismic hazard assessment for the Groningen gas field. *Netherlands Journal of Geoscience* **96**, s235–s245.
7. Edwards, B. & M. Ntinalexis (2021). Usable bandwidth of weak-motion data: application to induced seismicity in the Groningen Gas Field, the Netherlands. *Journal of Seismology*, doi: 10.1007/s10950-021-10010-7.
8. Ntinalexis, M., J.J. Bommer, E. Ruigrok, B. Edwards, R. Pinho, B. Dost, A.A. Correia, J. Uilenreef, P.J. Stafford & J. van Elk (2019). Ground-motion networks in the Groningen field: usability and consistency of surface recordings. *Journal of Seismology* **23**(6), 1233-1253.
9. J. Spetzler, J. & B. Dost (2017). Hypocentre estimation of induced earthquakes in Groningen. *Geophysical Journal International* **209**(1), 453–465.

Appendix A Evaluation of observed ground motions for the earthquake Zeerijp earthquakes based on GMM V6

The V7 GMM superseded and replaced the V6 GMM (Bommer *et al.*, 2019); the extensive additions, improvements and changes that the V7 GMM has in comparison to V6 are described in detail in Bommer *et al.* (2021). However, for completeness, and because the V6 GMM was used in the TNO-SDRA on which the current operational strategy for the Groningen field is based, we repeat the comparisons of Figures 13-17 for the V6 GMM in Figures A.1 to A.5 below.

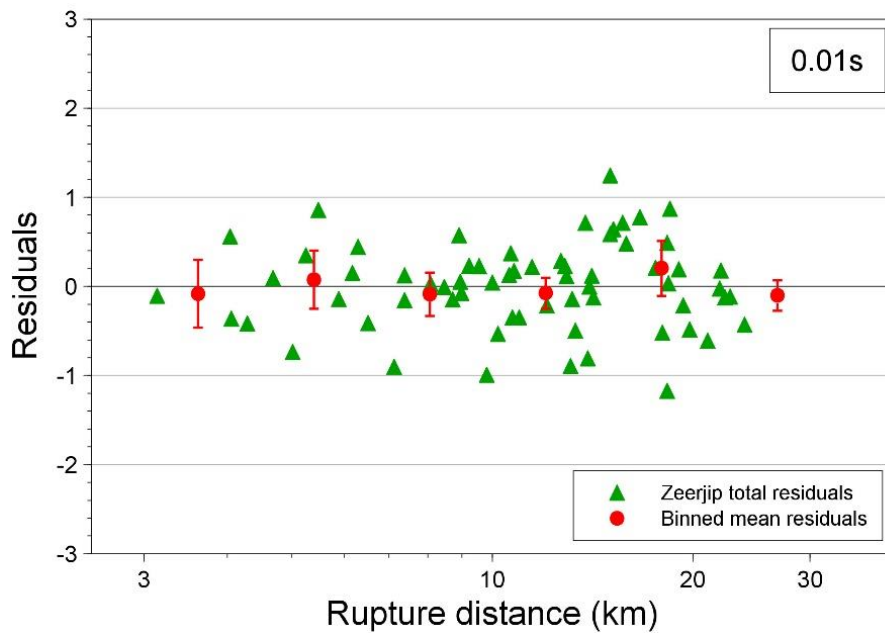


Figure A.1 Residuals of $S_a(T)$ with respect to the central branch of the V6 GMM at 0.01 seconds.

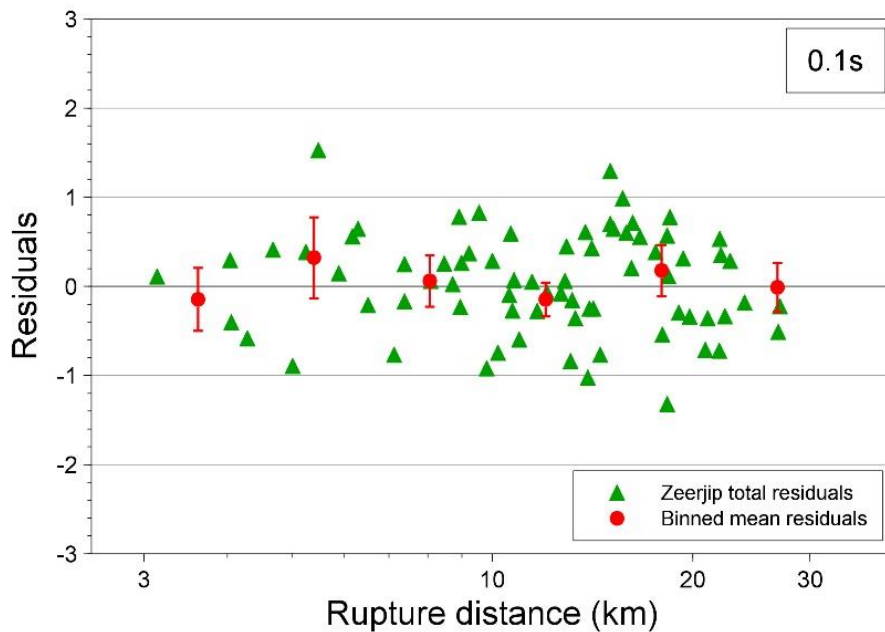


Figure A.2 Residuals of $S_a(T)$ with respect to the central branch of the V6 GMM at 0.1 seconds.

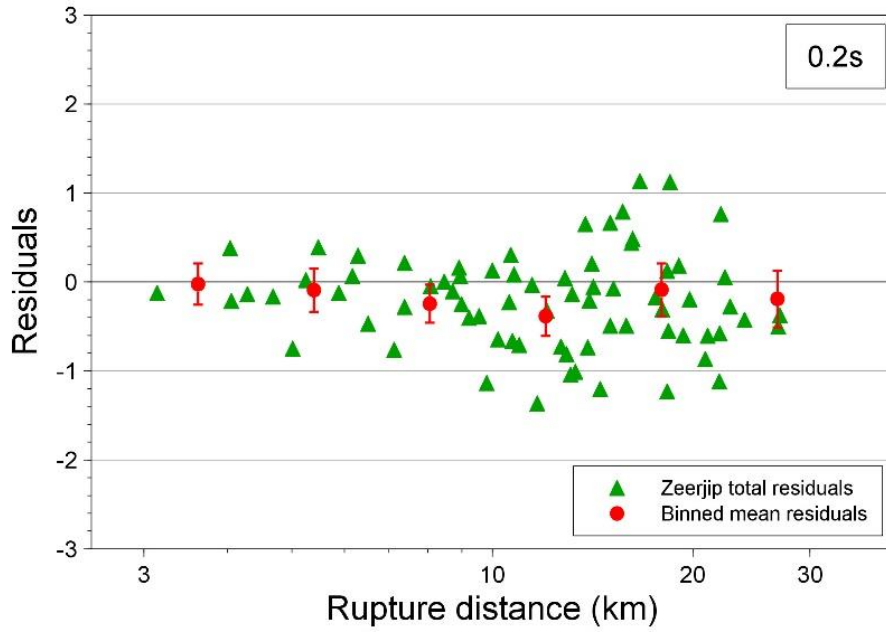


Figure A.2 Residuals of $S_a(T)$ with respect to the central branch of the V6 GMM at 0.2 seconds

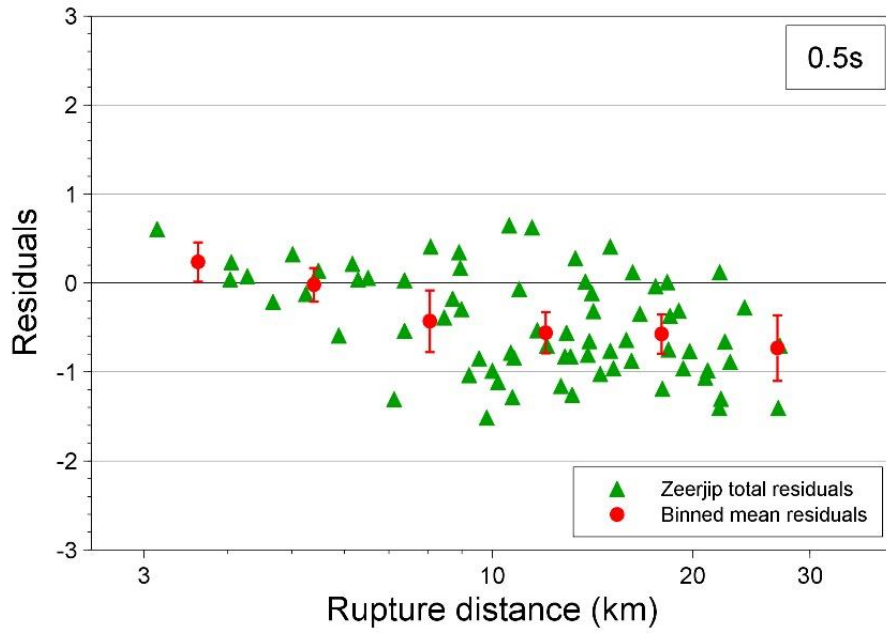


Figure A.3 Residuals of $S_a(T)$ with respect to the central branch of the V6 GMM at 0.5 seconds

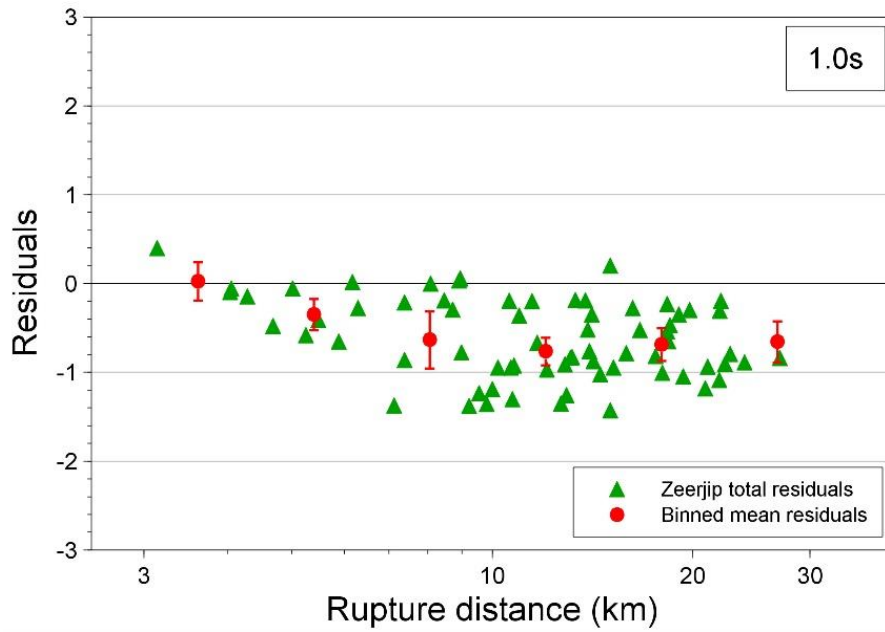


Figure A.4 Residuals of $S_a(T)$ with respect to the central branch of the V6 GMM at 1 second

The V6 residuals are reasonably well centred on the zero line at the shorter periods, up to and including 0.2 seconds. At longer periods, the V6 model has a clear tendency to over-estimate the ground-motions from this event. The V6 database was not included in Figures 18-22 for comparison, as it was processed differently to the records of this event.

Appendix B Evaluation of the hypocentre and the source mechanism of the earthquake with a magnitude of 3.2 near Garrelweer on 16th November

This appendix contains an evaluation of the recordings obtained with the seismic monitoring network operated by KNMI of the Garrelweer earthquake on the 16th November. The evaluation has been prepared by the Shell laboratory in Amsterdam using the automated Full-Wave-Form inversion.

This earthquake has been assigned number 58.



Event 58 - Garrelsweer

16 November 2021 00:46:48

16 November 2021

Induced Seismicity Taskforce

Disclaimer

- The results presented in this report have been automatically generated using an unconstrained full waveform, event location and moment tensor inversion workflow, developed by the Induced Seismicity Taskforce at Shell.
- These results have not been previously reviewed.
- For questions related to the results then you should contact:
 - Chris Willacy (Christopher.Willacy@Shell.com) or
 - Jan-Willem Blokland (Jan-Willem.Blokland@Shell.com)

Event summary

The event happened at:

Date	16 November 2021
Time	00:46:48.640000

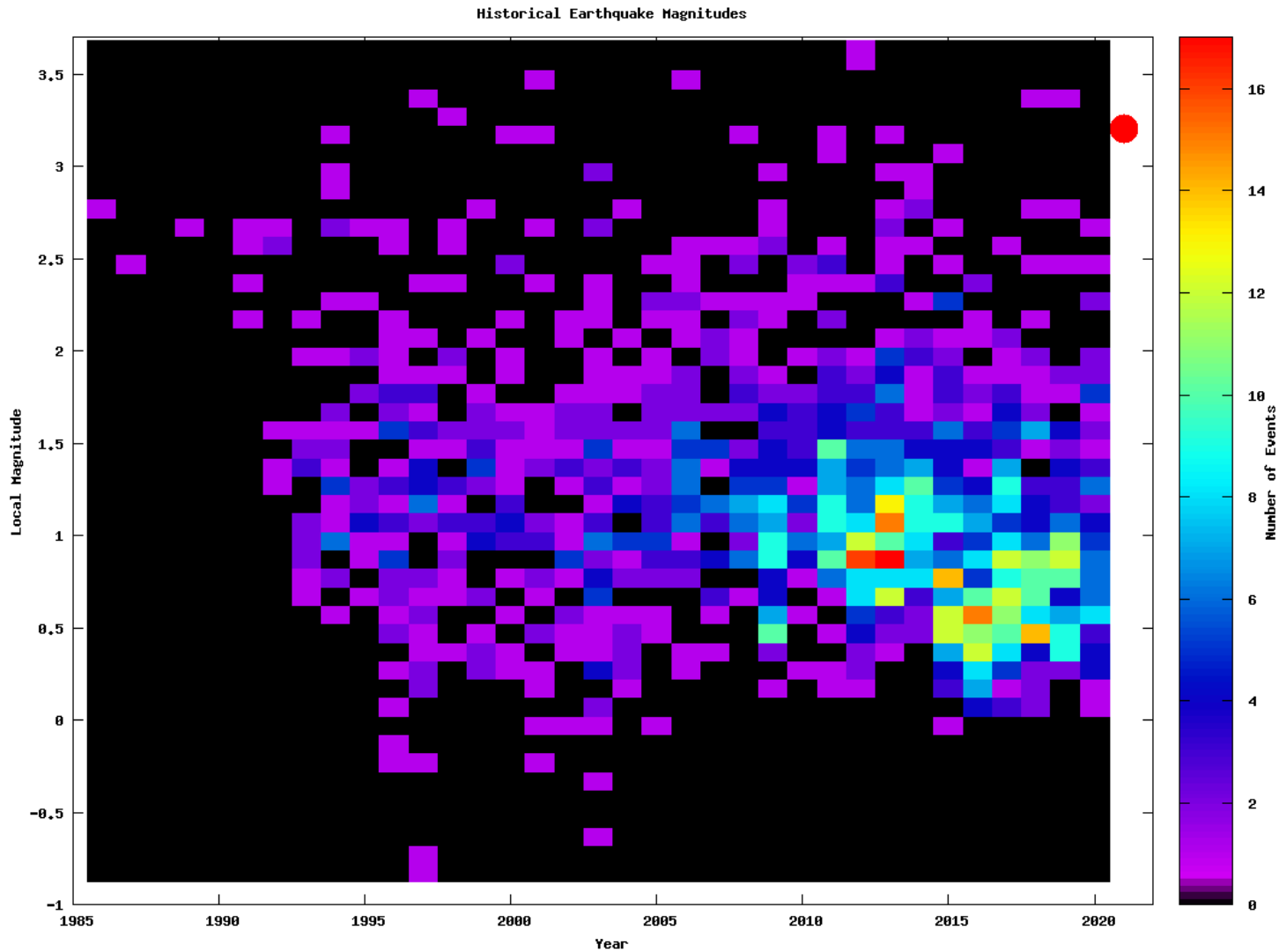
The event is located at:

Location	Garrelsweer
Northing (m)	592300
Easting (m)	245700
Depth (m)	3050

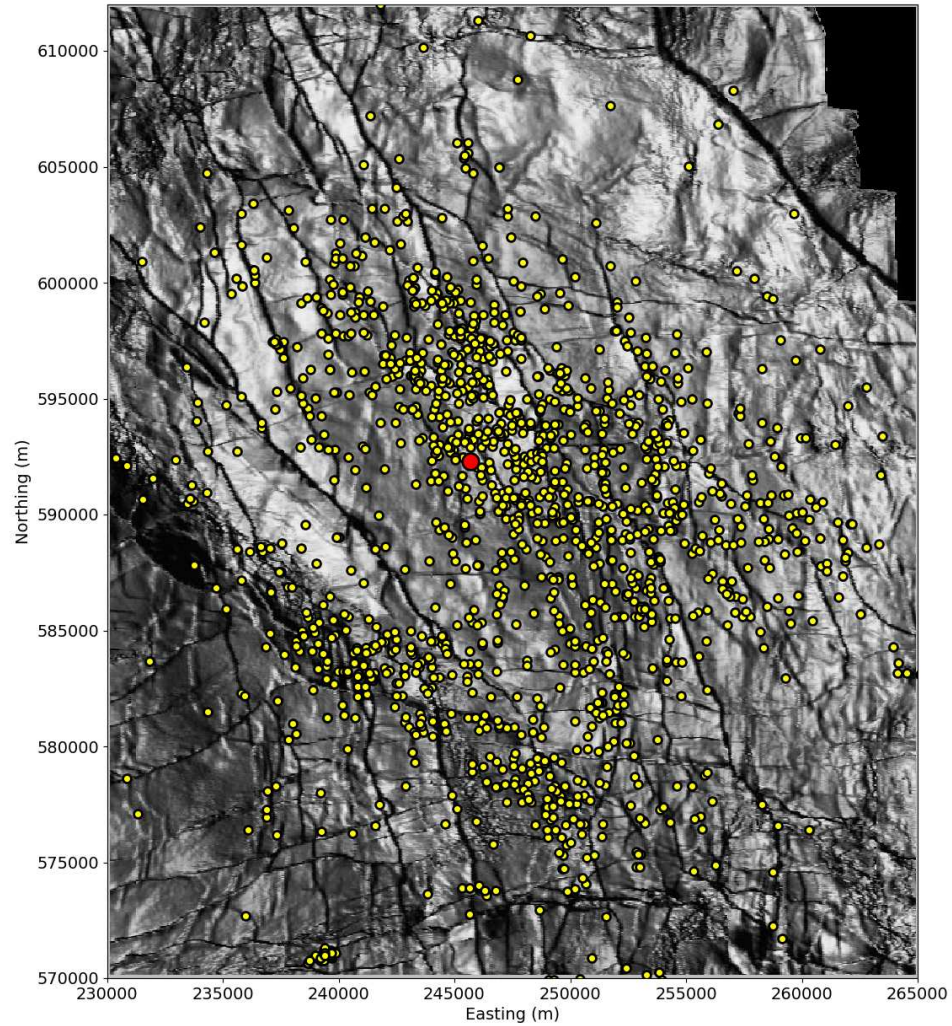
The source characteristics are:

	Solution 1	Solution 2
Strike angle (degree)	171.01	359.17
Dip angle (degree)	55.99	59.05
Rake angle (degree)	-97.69	-82.57
Isotropic (percentage)	-48.94	-48.94
CLVD (percentage)	24.88	24.88
Magnitude M_L	3.20	3.20

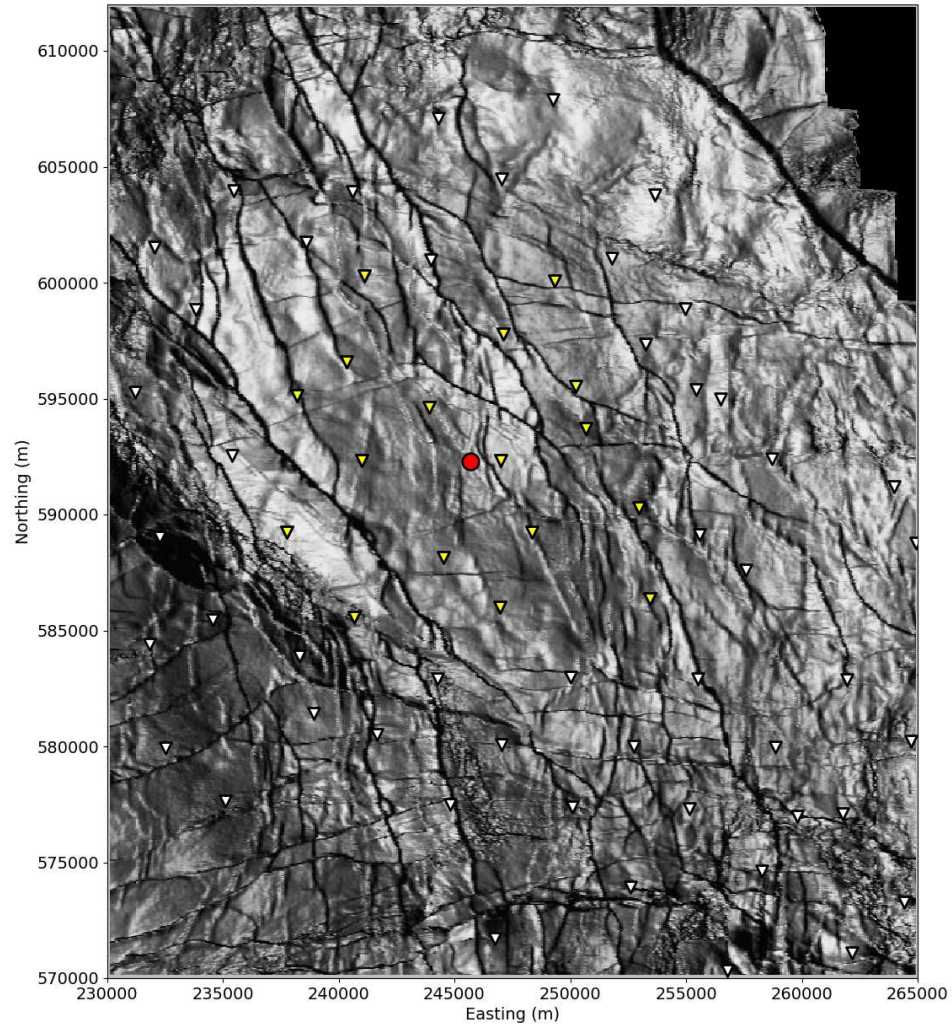
Magnitude summary



Regional and historical map

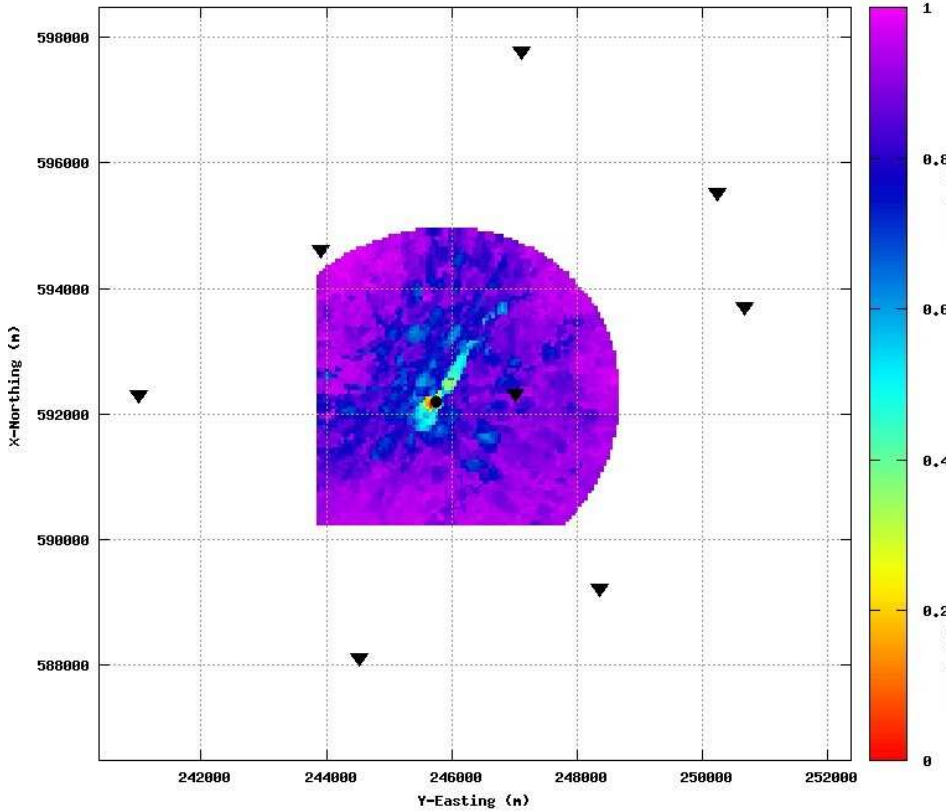


Event location - Map

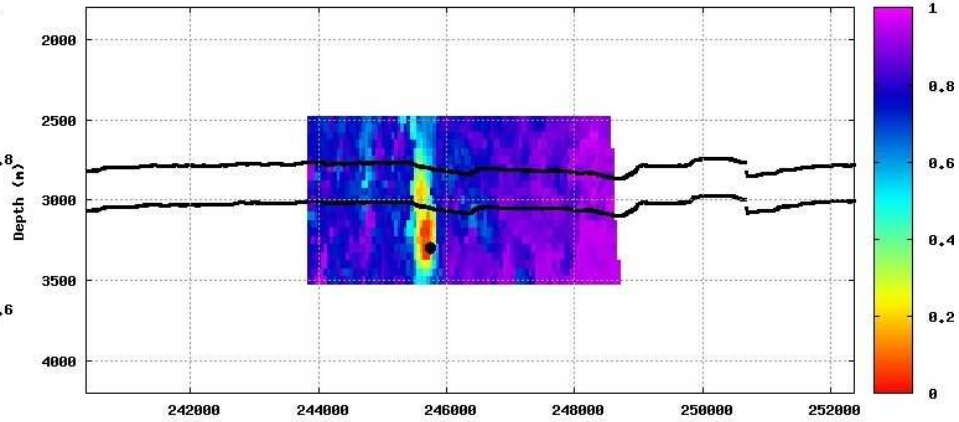


Event location and depth (initial)

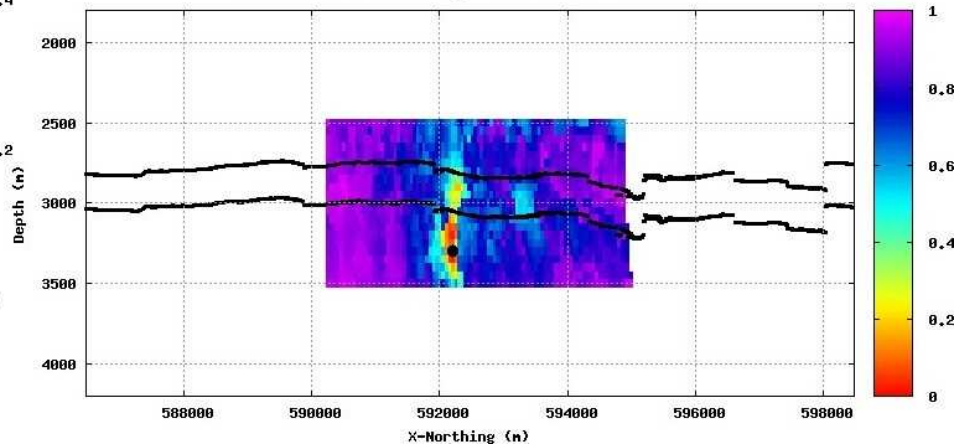
CORRVL, depth slice at ZSHT=3300n event:58 binnul:15



CORRVL, slice at X-Northing 592200n event:58 binnul:15

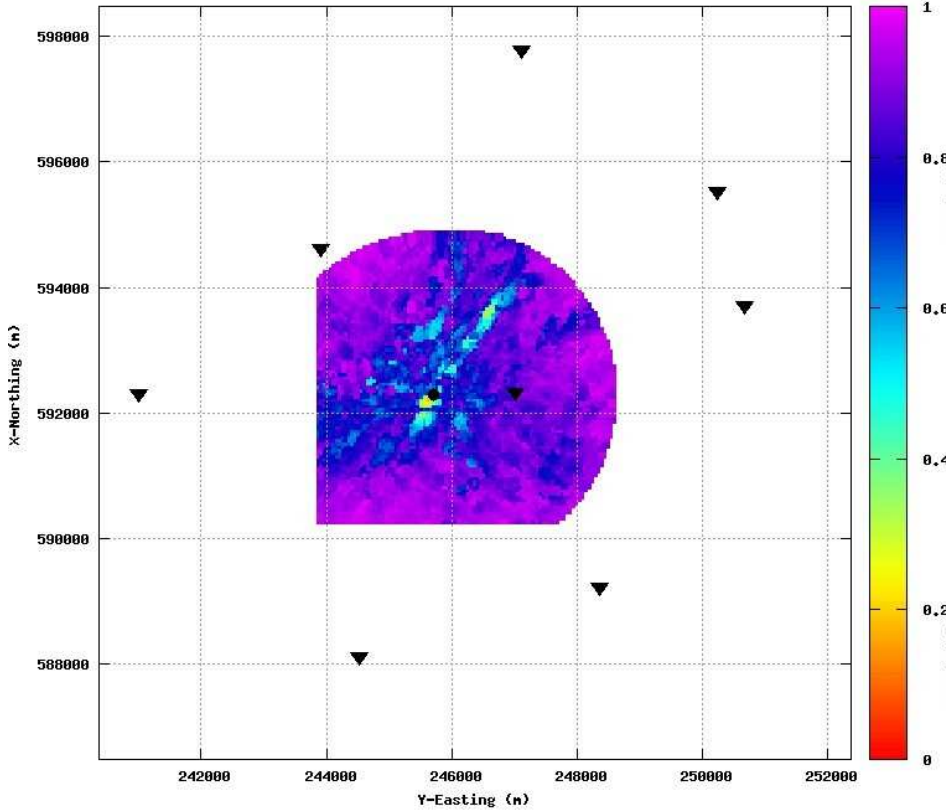


CORRVL, slice at Y-Easting 245750n event:58 binnul:15

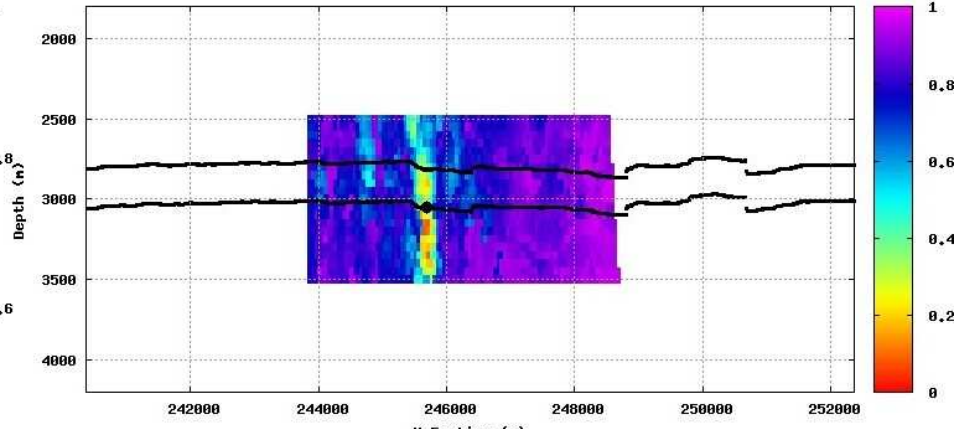


Event location and depth (alternative)

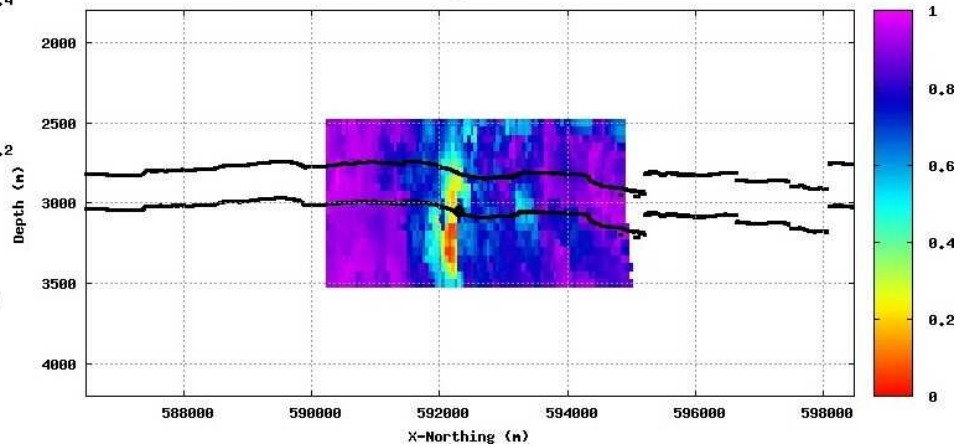
CORRVL, depth slice at ZSHT=3050n event:58 binnul:15



CORRVL, slice at X-Northing 592300n event:58 binnul:15

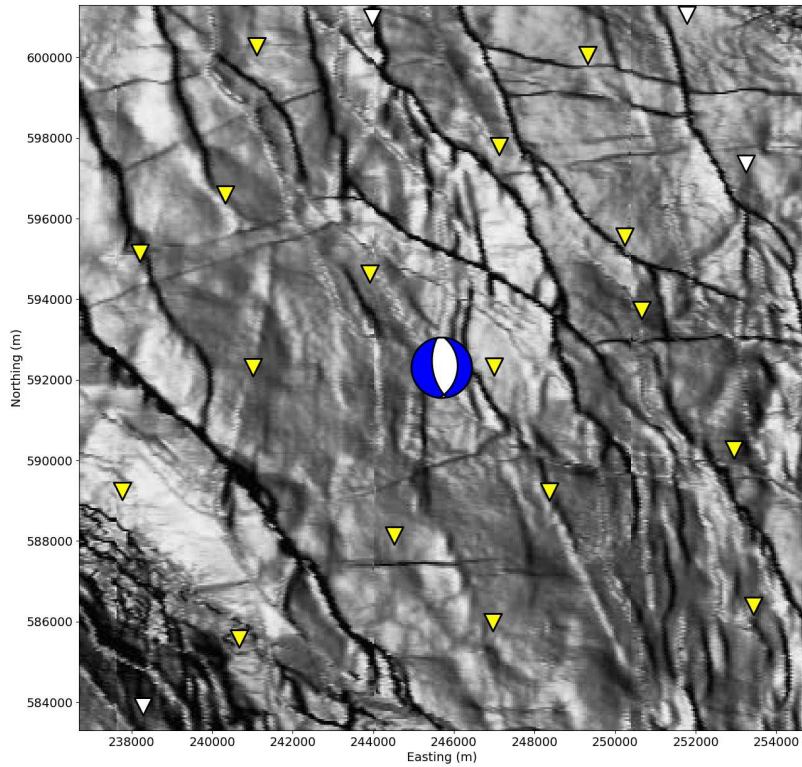


CORRVL, slice at Y-Easting 245700n event:58 binnul:15

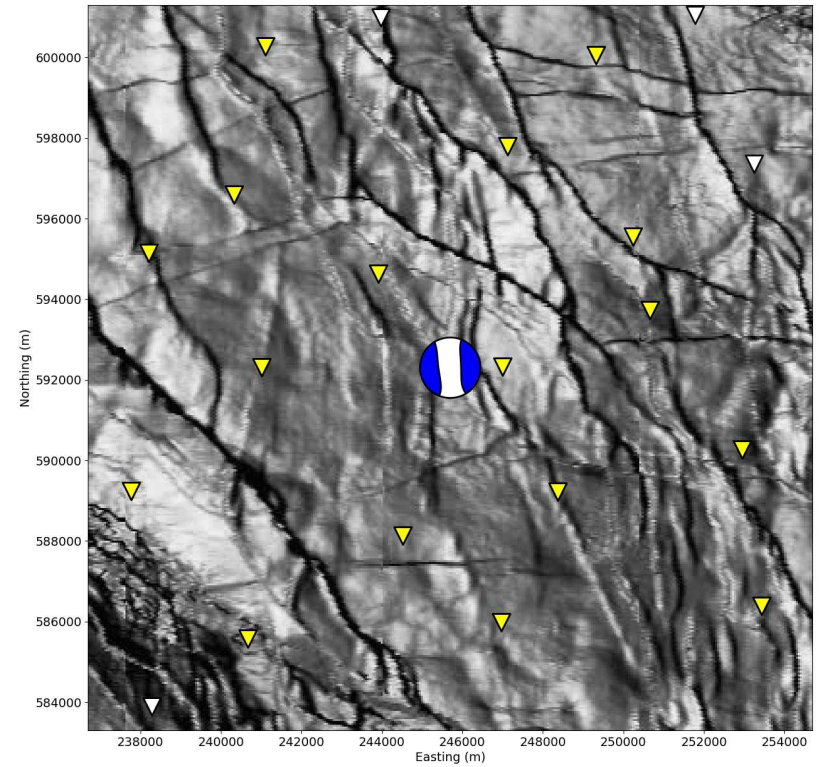


Moment tensor

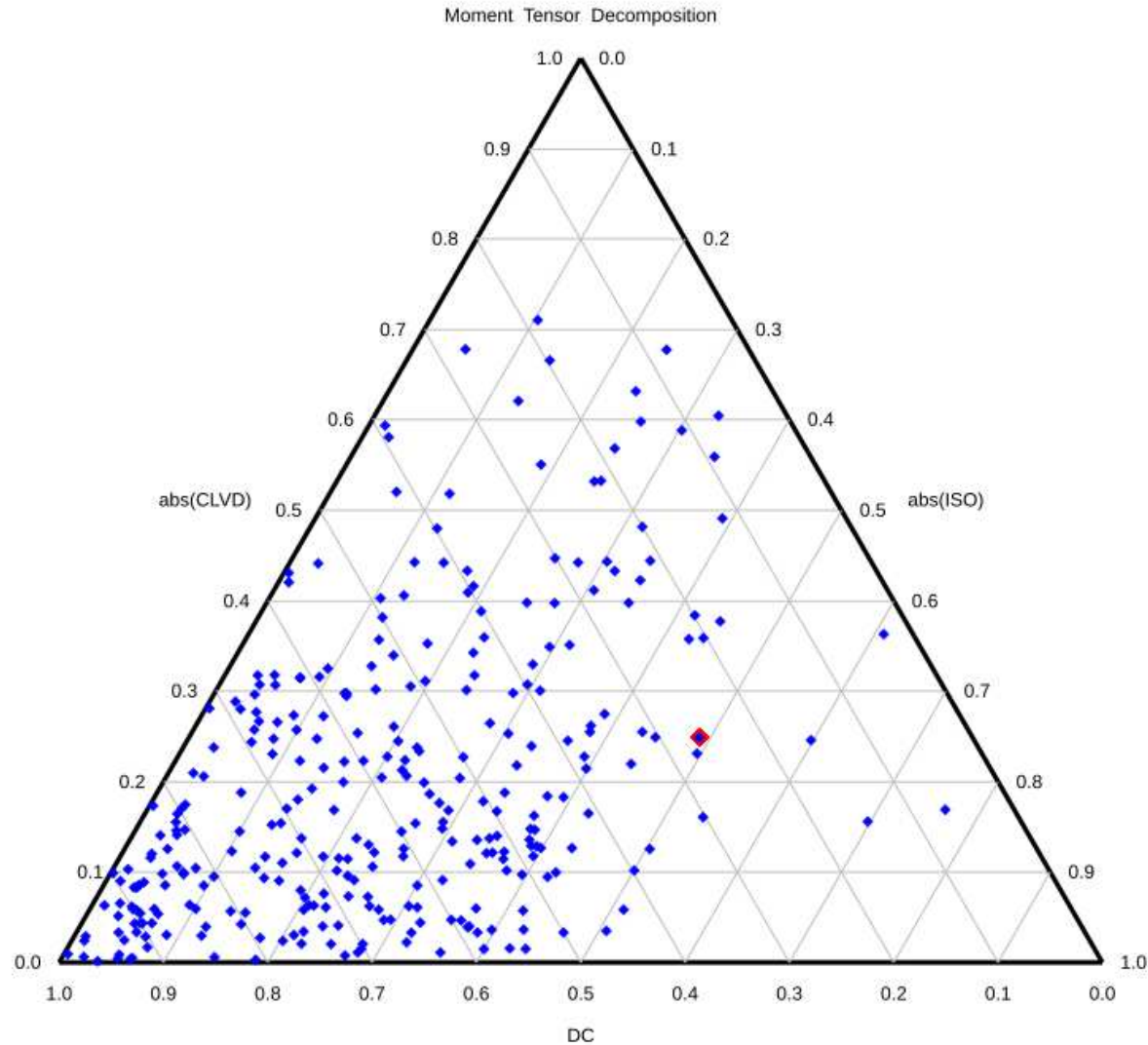
Double-coupled part



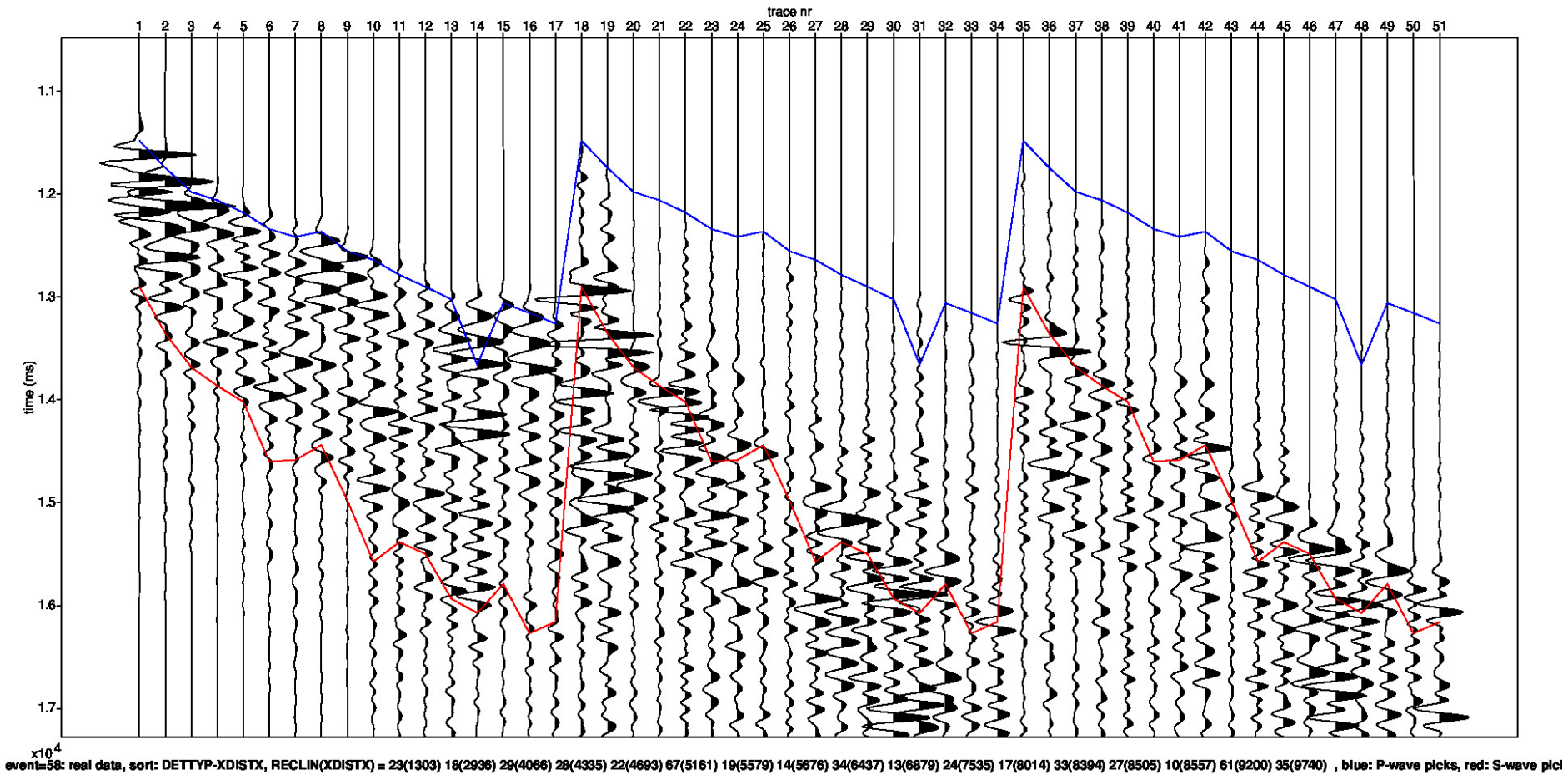
Full



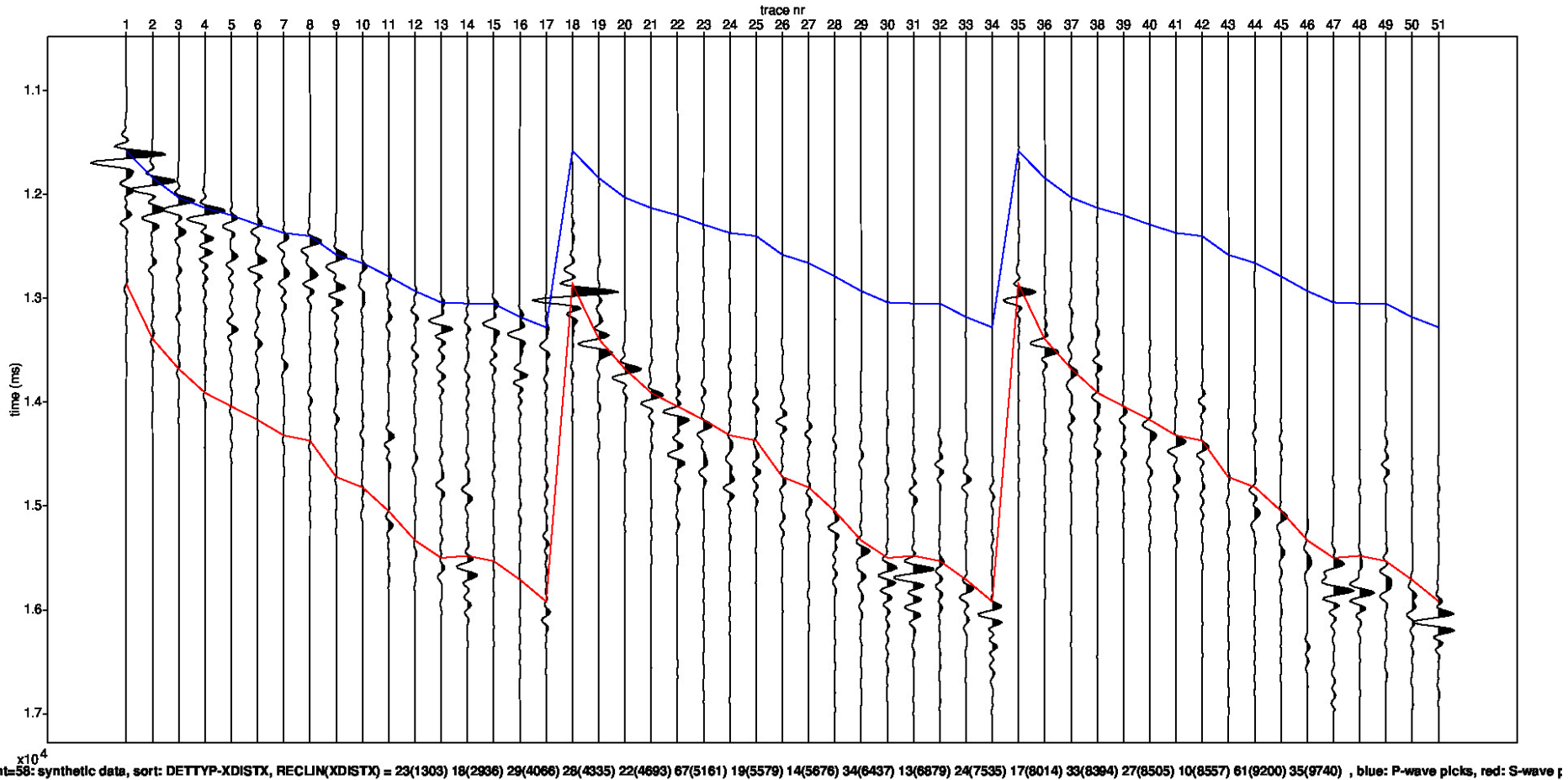
Moment Tensor: Decomposition



Field data traces



Modelled data traces



Appendix - Figure Captions

Page

- 3 Detailed parameter summary for the event. Both primary and secondary focal plane solutions are provided from the moment tensor inversion.
- 4 Magnitude summary. Prior years are displayed as a “heat map” where the number of events for a given magnitude is displayed per grid cell. The current event is displayed in red.
- 5 Regional map showing the historical events from KNMI (1986-2019) in blue and the location of the current event in red.
- 6 Event depth summary. Depths from our automatic workflow (2018-2020) are shown in blue and the current event depth is shown in red. The resolution of the vertical grid is 50m.
- 7 Event location details for the current event, superimposed on the top Rotliegend depth horizon. Station locations as shown as inverted triangles. Blue triangles are the actual stations used to locate the event whose epicentre is shown by the red dot.
- 8 QC displays extracted from the objective function for the initial event location. The colour attribute displayed is 1 minus the normalized cross correlation between observed and synthetic waveforms. Station locations are shown as black inverted triangles on the map and the event location is shown by the black dot (left plot). The west to east and north to south vertical profiles are shown on the right. The top and base reservoir are shown for reference as black lines.

Appendix - Figure Captions (continued)

Page

- 9 QC displays extracted from the objective function for the alternative event location. The colour attribute displayed is 1 minus the normalized cross correlation between observed and synthetic waveforms. Station locations are shown as black inverted triangles on the map and the event location is shown by the black dot (left plot). The west to east and north to south vertical profiles are shown on the right. The top and base reservoir are shown for reference as black lines.
- 10 Moment tensor inversion results for the event. The double couple portion of the moment tensor is shown on the left and the full moment tensor is displayed on the right. Station locations used in the inversion are shown as inverted triangles.
- 11 Ternary diagram showing the moment tensor decompositions into relative double-couple(DC), isotropic (ISO) and compensated linear vector dipole (CLVD) contributions. The automatic Shell events (2018-2020) are shown in blue and the current event is highlighted in red.
- 12 Observed traces for each station and each component. The automatic picks for the P- and S-waves are indicated by the blue and red lines respectively.
- 13 Modelled waveform data for each station and each component. The automatic picks for the P- and S-waves are indicated by the blue and red lines respectively.



